Neurotherapeutics
https://doi.org/10.1007/s13311-021-01074-x

ORIGINAL ARTICLE

N-Acylethanolamine-Hydrolyzing Acid Amidase Inhibition, but Not Fatty Acid Amide Hydrolase Inhibition, Prevents the Development of Experimental Autoimmune Encephalomyelitis in Mice

Pauline Bottemanne[1] · Owein Guillemot-Legris[1] · Adrien Paquot[1] · Julien Masquelier[1] · Michael Malamas[2] · Alexandros Makriyannis[2] · Mireille Alhouayek[1] · Giulio G. Muccioli[1]

Accepted: 13 June 2021
© The American Society for Experimental NeuroTherapeutics, Inc. 2021

Abstract

N-acylethanolamines (NAEs) are endogenous bioactive lipids reported to exert anti-inflammatory and neuroprotective effects mediated by cannabinoid receptors and peroxisome proliferator–activated receptors (PPARs), among others. Therefore, interfering with NAE signaling could be a promising strategy to decrease inflammation in neurological disorders such as multiple sclerosis (MS). Fatty acid amide hydrolase (FAAH) and *N*-acylethanolamine-hydrolyzing acid amidase (NAAA) are key modulators of NAE levels. This study aims to investigate and compare the effect of NAAA inhibition, FAAH inhibition, and dual inhibition of both enzymes in a mouse model of MS, namely the experimental autoimmune encephalomyelitis (EAE). Our data show that NAAA inhibition strongly decreased the hallmarks of the pathology. Interestingly, FAAH inhibition was less efficient in decreasing inflammatory hallmarks despite the increased NAE levels. Moreover, the inhibition of both NAAA and FAAH, using a dual-inhibitor or the co-administration of NAAA and FAAH inhibitors, did not show an added value compared to NAAA inhibition. Furthermore, our data suggest an important role of decreased activation of astrocytes and microglia in the effects of NAAA inhibition on EAE, while NAAA inhibition did not affect T cell recall. This work highlights the beneficial effects of NAAA inhibition in the context of central nervous system inflammation and suggests that the simultaneous inhibition of NAAA and FAAH has no additional beneficial effect in EAE.

Keywords Lipid mediator · *N*-palmitoylethanolamine · PEA · Neuroinflammation · Demyelination · *N*-acyltaurine

Introduction

Multiple sclerosis (MS) is a neurological disorder characterized by an autoimmune inflammatory response associated with immune cell infiltration across the blood brain barrier leading to gliosis, demyelination, and neuroaxonal degeneration. Ultimately, this leads to the disruption of neuronal signaling and, as a consequence, to heterogeneous symptoms ranging from visual disorders to motor impairments [1]. As numerous lipid mediators modulate inflammatory and immune processes, they appear as interesting strategies to tackle the disease [2–5].

N-acylethanolamines (NAEs) are bioactive lipids that have been studied for many years due to their pro homeostatic properties. Among their properties that could be interesting in the context of MS, NAEs are described to exert anti-inflammatory and neuroprotective effects [6–9]. Although *N*-arachidonoylethanolamine (anandamide, AEA) and *N*-oleoylethanolamine (OEA) have been shown to exert neuroprotective effects [6, 10, 11], the implication of *N*-palmitoylethanolamine (PEA) in (neuro)inflammation has been more thoroughly investigated. For instance, PEA administration was demonstrated to reduce inflammation and to exert neuroprotective effects in murine models of Alzheimer's disease [7, 12] and Parkinson's disease [13, 14]. At the molecular level, using antagonists and knockout mice, PEA was shown to exert most of its effects through interaction with the nuclear peroxisome proliferator–activated receptor-α (PPARα) [7, 12, 14]. Experiments have also been conducted to investigate the effects of PEA in models of MS

✉ Giulio G. Muccioli
giulio.muccioli@uclouvain.be

[1] Bioanalysis and Pharmacology of Bioactive Lipids Research Group, Louvain Drug Research Institute, UCLouvain, Université catholique de Louvain, B1.72.01, Av. E. Mounier 72, 1200 Bruxelles, Belgium

[2] Center for Drug Discovery and Departments of Chemistry and Chemical Biology and Pharmaceutical Sciences, Northeastern University, Boston, MA 02115, USA

Published online: 07 July 2021

[15, 16]. PEA administration was shown to decrease the clinical score and inflammation in murine models of the pathology [15, 16]. Of note, in patients, we have shown that PEA oral treatment (used as adjuvant to interferon-β1a) was able to decrease both pain and circulating pro-inflammatory cytokines, even though it did not improve their clinical symptoms [17].

Another important experimental approach to study the effects of NAEs is to increase their endogenous levels by inhibiting their hydrolytic enzymes. Two enzymes are responsible for NAE hydrolysis, the fatty acid amide hydrolase (FAAH), and the *N*-acylethanolamine-hydrolyzing acid amidase (NAAA) [18]. Even though these enzymes exert the same role, they differ in terms of biochemical properties, subcellular localization, and substrate preference among the NAEs [18–21].

In the experimental autoimmune encephalomyelitis (EAE) model of MS, FAAH inhibition with the potent and irreversible inhibitor URB597 did not exert beneficial effects [22]. However, the involvement of FAAH in EAE pathogenesis remains controversial. Indeed, using knockout mice, one study showed a beneficial effect of FAAH deletion on EAE disease progression [23]. In another study, FAAH deletion did not decrease demyelination or leukocyte infiltration in the white matter of the spinal cord at the peak of disease, but it improved the clinical score at later stages of the disease compared to wild type C57BL/6 mice [22]. However, both FAAH deletion and FAAH inhibition were shown to reduce spasticity in Biozzi ABH mice developing EAE [24]. However, the effects of NAAA inhibition are less studied in this context. One study reported that the administration of a NAAA inhibitor in EAE mice delays the onset of the disease and reduces its severity [25].

Even though both NAAA and FAAH are important enzymes controlling NAE metabolism, there has been no comparison of the effect of inhibiting FAAH and NAAA on MS in the same setting. Therefore, the aim of our study was to compare directly the effects of FAAH and NAAA inhibition, as well as the dual inhibition of these enzymes, in the same EAE model. We also wanted to test new and improved NAAA and NAAA-FAAH dual inhibitors (AM11095 and AM11078, respectively) along with the widely used and well characterized FAAH inhibitor, PF-3845. To gain additional insight on how NAAA inhibition was beneficial in the EAE model, we assessed the effect of the inhibitors in an ex vivo model of neuroinflammation and in a T cell recall assay.

Material and Methods

Animals

C57BL/6J female mice (Janvier Labs), 8 to 9 weeks old, were used in all experiments. They were housed in filter-top cages under controlled conditions of temperature (20–22 °C) and artificial light (12 h dark/12 h light) and supplied with drinking water and food ad libitum. All efforts were made to minimize suffering. All animal experiments were performed in accordance with the guidelines of the local ethics committee and in accordance with European directive 2010/63/EU, which was transformed into the Belgian Law of May 29, 2013 regarding the protection of laboratory animals. The local ethics committee of the Université catholique de Louvain reviewed and approved the experimental protocols (study agreement 2017/UCL/MD/024, laboratory agreement LA1230635).

Drugs and Reagents

The NAAA inhibitor (AM11095) and dual NAAA-FAAH (AM11078) inhibitor were synthesized in the laboratory of A. Makriyannis [26, 27]. AM11095 inhibits NAAA activity with a half-maximal inhibitory concentration (IC_{50}) value of 18 nM, while having limited effect on FAAH activity ($IC_{50} > 100$ µM). AM11078 inhibits NAAA and FAAH activity with an IC_{50} value of 21 nM and 5 nM, respectively. PF-3845 (*N*-3-pyridinyl-4-[[3-[[5-(trifluoromethyl)-2-pyridinyl]oxy]phenyl]methyl]-1-piperidinecarboxamide) was purchased from Tocris Bioscience (R&D Systems Europe Ltd., Abingdon, UK). FluoroMyelin Green was purchased from Invitrogen. Lipopolysaccharides (LPS) from *Escherichia coli* (O55:B5) and Luxol fast blue (solvent blue 38; LFB) were purchased from Sigma-Aldrich (Diegem, Belgium). The Hooke kit EK-2110 was used to induce EAE while the kit CK-0111 was used for the control mice and the $MOG_{35–55}$ antigen (DS-0111) was used for cell recall in vitro (Hooke Laboratories, Lawrence, MA, USA).

EAE Model

EAE Induction

EAE was induced in C57BL/6J female mice using a kit from Hooke Laboratories (Lawrence, MA, USA) following the manufacturer's instructions. Briefly, after acclimation, mice were immunized by a subcutaneous injection with 100 µg of $MOG_{35–55}$ (a myelin oligodendrocyte glycoprotein peptide) in complete Freund's adjuvant (CFA; containing 2.5 mg/mL killed Mycobacterium tuberculosis (H37Ra)) at two sites on the back (100 µL/injection). Then, pertussis toxin (PTX) in phosphate buffered saline (PBS) (80 ng/100 µL) was administered intraperitoneally 2 h after immunization and again the following day [28]. Control mice received CFA emulsion on day 0 and vehicle of PTX on days 0 and 1.

Treatments

The FAAH inhibitor PF-3845 (10 mg/kg) was administered once daily [29] while the NAAA inhibitor AM11095 (15 mg/

kg), the dual NAAA-FAAH inhibitor AM11078 (15 mg/kg) or the vehicle alone were administered intraperitoneally twice daily starting, depending on the study, 3 days post immunization or when 25% of the mice had at least a limp tail tip as clinical sign. The inhibitors were administered in a vehicle consisting of saline-DMSO-Tween® 80 (18:1:1, v/v/v). AM11095 and AM11078 dose and scheme of administration were determined based on previous studies in the laboratory.

EAE Monitoring

Mice were weighed daily and monitored for neurological symptoms associated with a progressive paralysis of the tail and hind legs. The scoring was based on the protocol from Hooke Laboratories: score 0: no sign of the disease, the tail is erect when picked up at the base, and locomotor activity is intact compared to non-immunized mice; score 0.5: when picked up at the base, the tip of the tail is limp; score 1: when picked up at the base, the tail is limp; score 1.5: the tail is limp and walking is slightly wobbly with a weakness in one hind leg; score 2: when picked up at the base, the tail is limp and legs are not spread apart or the mouse presents signs of head tilting, both symptoms are associated with poor balance; score 2.5: the tail is limp, the two hind legs are weak or no movement in one leg or the mouse presents signs of head tilting with occasional fall over; score 3: the tail is limp with complete or almost complete paralysis of hind legs (legs are able to paddle but not to move forward of the hind hip); score 3.5: the tail is limp with complete paralysis of hind legs (hind quarters are flat and the mouse is unable to right itself when put on the side); and score 4: the tail is limp with complete paralysis of hind legs associated with weakness or partial paralysis in the front legs.

For the preliminary study (shown in Fig. 1), mice were sacrificed when they reached a clinical score of 0.5–1 or 3.5–4 in order to constitute different groups of mice based on their score. For the studies on enzyme inhibition, mice were euthanized 30 days post immunization and 1 h after the last injection of inhibitors or vehicle. In all studies, at the moment of sacrifice, tissues were carefully resected and stored in the appropriate manner for further analysis.

T Cell Recall Ex Vivo

For this ex vivo assay, mice were immunized with $MOG_{35–55}$ in CFA and treated with vehicle or the different inhibitors from day 3 post immunization (as described above) to day 14. On day 14, a single cell suspension was isolated from the spleen and from the draining lymph nodes of the mice and cultured for 48 h in the presence or not of $MOG_{35–55}$ (20 µg/mL) following the protocol from Hooke Laboratories, in RPMI 1640 supplemented with 10% fetal bovine serum, 10 mM HEPES, 2 mM L-glutamine, MEM non-essential amino acids, 1 mM sodium pyruvate, 55 µM 2-mercaptoethanol, 100 units/mL penicillin, and 100 µg/mL streptomycin. The medium without $MOG_{35–55}$ was used as negative control. mRNA expression of inflammatory markers was measured by RT-qPCR.

Primary Astrocyte and Microglia Co-culture and Treatment

The primary astrocyte and microglia co-culture was set up as previously described [30, 31]. Briefly, cerebral cortices were recovered from C57BL/6J mice pups. After mechanical dissociation of the tissues the resulting suspension was centrifuged and resuspended in DMEM-F12 media (containing 10% fetal bovine serum, 100 units/mL penicillin, and 100 µg/mL streptomycin). Cells were then seeded in poly-lysine pre-coated flasks (two pups per flask) and incubated

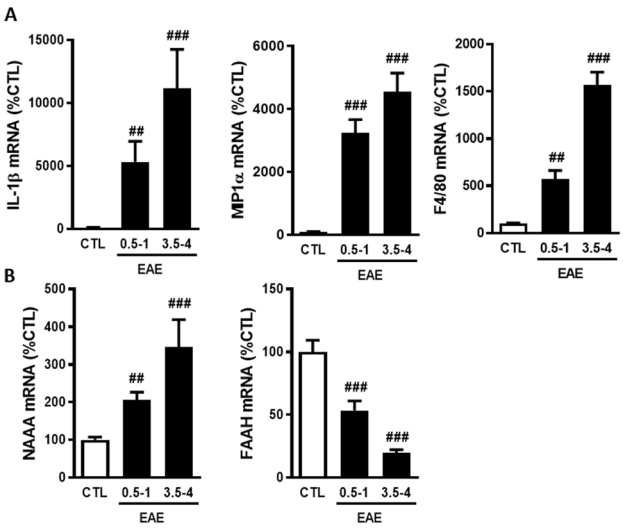


Fig. 1 Correlation between mRNA expression of enzymes hydrolyzing *N*-acylethanolamines and the severity of EAE. EAE was induced in C57BL/6J female mice by immunization with $MOG_{35–55}$ in CFA on day 0 and PTX injections on days 0 and 1. Control (CTL) mice received CFA emulsion on day 0 and vehicle of PTX on days 0 and 1. Mice were killed at different stages of the disease. 0.5–1 corresponds to a low EAE clinical score and 3.5–4 to a high EAE clinical score. mRNA expression of **(A)** pro-inflammatory markers (IL-1β, MIP1α, F4/80) and (**B**) enzymes hydrolyzing *N*-acylethanolamines (NAAA and FAAH) was measured in the spinal cord of EAE mice by RT-qPCR using RPL19 as reference gene. **(C)** Spearman correlations between mRNA expression of inflammatory markers and mRNA expression of NAAA and FAAH in the spinal cord was assessed from the data in **A** and **B** (r value and significance are reported). Data represent mean ± SEM and are expressed as percentage of the control (CTL) group (n = 10–19 mice per group) $^{\#\#}p < 0.01$; $^{\#\#\#}p < 0.001$ vs. the control group

for 2 weeks. The medium was changed twice, on day 5 and day 10. After 14 days of culture, the flasks were trypsinized and cells were seeded in poly-lysine pre-coated petri dishes for NAE quantification (10^7 cells/petri) and 24 well plates for RT-qPCR assay (200,000 cells/well). Following overnight incubation, the cells were incubated with enzyme inhibitors (10 µM) in a fresh culture medium for 1 h and activated or not with LPS (10 or 100 ng/mL) or with a combination of IFNγ (20 ng/mL) and TNF-α (50 ng/mL) for 5 h for NAE quantification and for 8 h for macrophage activation assessment [32]. For all experiments, a control condition was performed where the cells were only incubated with vehicle (DMSO, 0.05%).

RNA Extraction and Real-time qPCR

Total RNA was extracted using the TriPure® reagent (Roche) according to the manufacturer's instructions. cDNA was synthesized using a reverse transcription kit (RT GoScript mix, Promega). qPCR was performed with a StepOnePlus instrument and software (Applied Biosystems). The products were analyzed by performing a melting curve at the end of the PCR [33]. Data are normalized to the 60S ribosomal protein L19 (RPL19) mRNA expression. Primer sequences for qPCR are listed in Table 1.

Multiplex

The spinal cord was homogenized in PBS-0.05% TritonX-100 using a TissueLyser II (Qiagen). Total protein concentration was determined using the DC protein assay (Bio-Rad) following the manufacturer's instructions. Following dilution of the spinal cord homogenates (45 µg protein/sample), cytokines and chemokines were quantified using a Bio-Plex Multiplex kit (Bio-Rad, Nazareth, Belgium) and measured by using Luminex technology (Bio-Plex 200; Bio-Rad) or using a U-Plex assay from (Mesoscale Discovery, MD, USA) with an electrochemiluminescence detection system, following the manufacturers' instructions.

Histology

Spinal cords were hydro-extruded and fixed in 4% PFA for 48 h, transferred in a 15% sucrose solution for 24 h and then in a 30% sucrose solution for 24 h, embedded in O.C.T. compound (VWR), and finally kept at − 80 °C. Cryosections were cut using a cryostat. The lumbar region of the spinal cord was serially sliced (coronal sections) at a thickness of 20 µm (for LFB staining) or 30 µm (for immunofluorescence and Fluoromyelin Green staining). Each slide analyzed contained five to six spinal cord slices.

Table 1 Primer sequences

Gene/product	Forward primer (5′ to 3′)	Reverse primer (5′ to 3′)	Accession number	Product length
Atf3/ATF3	CGCCATCCAGAATAAACACC	CCTTCAGCTCAGCATTCACA	NM_007498.3	248
Adgre1/F4/80	TGACAACCAGACGGCTTGTG	CAGGCGAGGAAAAGATAG	NM_010130.4 NM_001355722.1 NM_001355723.1	60
Faah/FAAH	GAGATGTATCGCCAGTCCGT	ACAGGCAGGCCTATACCCTT	NM_010173.5	287
Foxp3/FOXP3	GTTCCTTCCCAGAGTTCTTCC	CATCGGATAAGGGTGGCATAG	NM_001199347.1 NM_054039.2 NM_001199348.1	88
Il1b/IL-1β	TGTCTTTCCCGTGGACCTTC	CCAGCAGGTTATCATCATCATCCC	NM_008361.4	111
Il10/IL-10	TTCTTTCAAACAAAGGACCAG	ACCCAAGTAACCCTTAAAGT	NM_010548.2	78
Il17a/IL-17A	GACTACCTCAACCGTTCCAC	CACTGAGCTTCCCAGATCAC	NM_010552.3	89
Il22/IL-22	GCTCAGCTCCTGTCACATC	CCCAATCGCCTTGATCTCTC	NM_016971.2 NM_054079.2	112
Il6/IL-6	ACAAGTCGGAGGCTTAATTACACAT	TTGCCATTGCACAACTCTTTTC	NM_031168.2 NM_001314054.1	72
Ifng/IFNγ	GTTTGAGGTCAACAACCCACAG	GCTTCCTGAGGCTGGATTC	NM_008337.4	95
Nos2/*iNOS*	AGGTACTCAGCGTGCTCCAC	GCACCGAAGATATCTTCATG	NM_010927.4 NM_001313921.1 NM_001313922.1	190
Naaa/NAAA	GGTTTTATCCCTGTTTCCTGTTTAT	TTTTTGACAATACATCACCTTCAGCT	NM_001163687.1 NM_025972.4	126
Ccl3/MIP1α	AGATTCCACGCCAATTCATC	CTCAAGCCCCTGCTCTACAC	NM_011337.2	223
Rpl19/RPL19	TGACCTGGATGAGAAGGATGAG	CTGTGATACATATGGCGGTCAATC	NM_009078.2 NM_001159483.1	88
Tnf/TNF-α	CTACTGAACTTCGGGGTGATC	TGAGTGTGAGGGTCTGGGC	NM_013693.3 NM_001278601.1	94

LFB Staining

LFB stain was used to assess myelin loss. Briefly, cryosections were immersed in isopropanol and then stained in LFB for 8 h at room temperature. The excess stain was removed in an isopropanol bath and then a solution of lithium carbonate was used for differentiation before mounting the slides. Images were acquired using a Leica SCN400 slide scanner.

Immunofluorescence

Cryosections were washed in PBS containing 0.2% triton (PBS-T), incubated with a blocking solution (normal goat serum (NGS) 4% in PBS-T) and incubated overnight at 4 °C with primary antibodies: rabbit anti-Iba1 (1:500, Wako Laboratory Chemicals, ref: 019–19,741), direct rat anti-GFAP (1:250, Merck, ref: C9205), or rabbit anti-CD3 (1:250, Dako, ref: A0452) [28]. All primary antibodies were diluted in PBS-T containing 2%-NGS and incubated overnight at 4 °C. The following day, slides were washed 3 times for 10 min in PBS-T and then incubated with the fluorescent secondary antibody Alexa-Fluor 488 conjugated goat anti-rabbit polyclonal (1:250, Invitrogen, ref: 35553) or the Alexa-Fluor 647 conjugated goat anti-rabbit polyclonal (1:250, Invitrogen, ref: A32733) in PBS-T containing 2% NGS overnight at 4 °C. Slides were then washed three times for 10 min with PBS-T and incubated with nuclear stain (DAPI). After rehydration in PBS, sections were incubated in Fluoromyelin Green (1:300, Invitrogen, ref: F34651) following the manufacturer's instructions to assess lesions in the spinal cord [28]. Image acquisition was performed using a Panoramic P250 Flash III slide scanner (3DHISTECH).

Staining Quantification

Image analysis was performed by a researcher, blinded to the group allocation, using ImageJ software (https://imagej.nih.gov/ij/) or CaseViewer (3DHISTECH). For the percentage of area occupied, according to the marker studied, an automatic thresholding or a manual method was applied. Five to six spinal cord slices were analyzed per animal and the mean of the values obtained for each slice was then calculated in order to generate a single value per animal.

N-Acylethanolamine Quantification

Samples (spinal cord, brain) were homogenized in dichloromethane (CH_2Cl_2, 8 mL). For cells, medium was discarded and the cells were recovered with PBS and placed in vials containing 8 mL of CH_2Cl_2. Then, methanol (MeOH, 4 mL) (containing butylated hydroxytoluene) was added to the mixture. For plasma, the samples (50 µL) were directly added to the organic solvents. After homogenization, deuterated internal standards were added. Following the addition of water (containing EDTA), the vials were shaken and sonicated in an ice bath. As previously reported, after centrifugation, the organic phase was recovered and purified by solid phase extraction [34]. The lipids of interest were recovered using hexane–isopropanol (7:3; v/v) and analyzed by UPLC-MS/MS.

The samples (1 µL) were injected on a Xevo TQ-S mass spectrometer equipped with an Acquity UPLC® class H (both from Waters). An Acquity UPLC® BEH C18 (2.1 × 50 mm; 1.7 µm, kept at 40 °C) column and a linear gradient (200 µL/min) between MeOH-H_2O-acetic acid (75:24.9:0.1; v/v/v) and MeOH-acetic acid (99.9:0.1; v/v) were used for the separation. A quantification and a qualification transition were optimized for the different NAEs and deuterated standards, and the MassLynx® software was used for data acquisition and processing. For each compound, the ratio between the area under the curve of the lipid and the area under the curve of the corresponding internal standard was used for data normalization. Calibration curves with a range going from 2.5 to 800 fmol (values on column) were also obtained in the same conditions. The obtained values were then normalized to the amount of biological matrices.

Statistical Analysis

GraphPad Prism (GraphPad Software) was used for statistical analysis. Results are expressed as mean ± SEM. Data were first tested for normality using the Shapiro–Wilk test. If the data were normally distributed, differences between treatments and vehicle were evaluated by one-way ANOVA with Dunnett's post hoc test. When the data deviated significantly from normality, a Kruskal–Wallis with Dunn' s post hoc test was used. For the T cell recall assay, differences between the groups were analyzed by a two-way ANOVA with Sidak post hoc test. For studies where only two groups were present (supplementary figures), differences were assessed using either a two-tailed unpaired Student's *t*-test or a two-tailed Mann–Whitney test. Statistical significance was taken when $p < 0.05$. The number of animals per group is specified in the figure legends.

Results

EAE Differently Affected NAAA and FAAH mRNA Expression

We induced EAE in C57BL/6J mice using an immunization with $MOG_{35–55}$. The clinical evolution of the disease followed the classical pattern reported for EAE in C57BL/6 mice [35, 36], while the control mice showed a normal behavior. In this

first study, we sacrificed the mice either at the first sign (clinical score 0.5–1) or at the peak (clinical score 3.5–4) of the disease. Mice from the control group were sacrificed at similar moments as the EAE mice. The EAE model is characterized by inflammation and immune cell infiltration in the spinal cord. We measured the mRNA expressions of a pro-inflammatory cytokine (IL-1β), of the chemokine MIP1α and of the myeloid marker F4/80. We found an increase of their expressions in the spinal cord of EAE mice compared to control mice (Fig. 1A). Then, we sought to assess the impact of the disease on the expressions of both NAE hydrolyzing enzymes. In the spinal cord of control mice, both FAAH mRNA and NAAA mRNA were expressed. We found FAAH to be more expressed than NAAA when comparing the ΔCt between the threshold cycle (Ct) of the gene of interest (FAAH or NAAA) and the threshold cycle of the reference gene for both enzymes (Fig. S1A). Interestingly, mRNA expressions of NAAA and FAAH were differently altered in the spinal cord of EAE mice. Indeed, NAAA mRNA levels were increased with the evolution of the pathology (clinical score) while FAAH mRNA expression was decreased (Fig. 1B). Additionally, we found the mRNA expressions of IL-1β, MIP1α, and F4/80 to be positively correlated with NAAA and negatively correlated with FAAH mRNA expression (Fig. 1C).

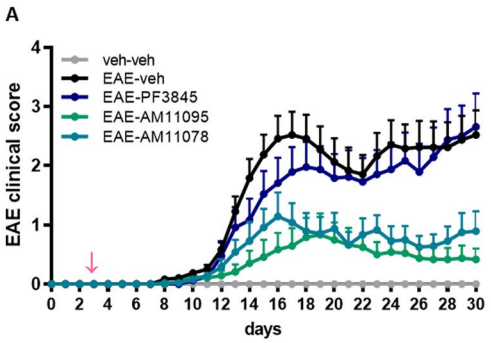
Mice Receiving the NAAA Inhibitor Were Less Sensitive to EAE

NAAA Inhibition and Dual NAAA-FAAH Inhibition, but Not FAAH Inhibition, Attenuated EAE Severity

Both FAAH and NAAA are important enzymes for the control of NAE levels [20, 37, 38]. Here we decided to compare, in the same study, the effect of their inhibition. We used AM11095 as NAAA inhibitor and PF-3845 as FAAH inhibitor [26, 27, 39]. Moreover, because the concomitant inhibition of NAAA and FAAH could offer an advantage over the inhibition of one of the enzymes, we also assessed the effects of AM11078, a dual NAAA–FAAH inhibitor [26].

Vehicle-treated EAE mice showed signs of the disease starting on day 12 post immunization and reached a mean maximal clinical score of 2.77 at the peak of the disease (Fig. 2A, B). Mice treated with daily administrations of the NAAA inhibitor, AM11095, from 3 days after induction of the disease to day 30, were either protected against EAE development or presented a delay in the mean day of onset compared to EAE mice. Indeed, 7 out of 12 mice treated with AM11095 remained free of disease (Fig. 2A, B). Moreover, the mice that developed the disease (mice were considered sick when they had limp tail) began to

Fig. 3 NAAA inhibition and dual NAAA-FAAH inhibition reduced glial cell activation and lymphocyte presence in the spinal cord of EAE mice. EAE was induced in C57BL/6J female mice by immunization with $MOG_{35–55}$ in CFA on day 0 and PTX injections on days 0 and 1. The NAAA inhibitor, AM11095 (15 mg/kg, b.i.d.), the dual NAAA-FAAH inhibitor, AM11078 (15 mg/kg, b.i.d.), the FAAH inhibitor, PF-3845 (10 mg/kg, q.d.), or vehicle (veh) were administered intraperitoneally, starting from day 3 after EAE induction to day 30. Control (CTL) mice received CFA emulsion on day 0 and vehicle of PTX on days 0 and 1. Mice were killed on day 30 post immunization. Representative photomicrographs and quantification of the area occupied by (**A**) Iba-1 positive cells (microglia), (**B**) GFAP positive cells (astrocytes), and (**C**) CD3 positive cells (T lymphocytes) of the spinal cord expressed as percentage (i.e., (marker-positive area of the ventral white matter / total area of the ventral white matter) × 100). The scale bar represents 20 µm. Data are reported as mean ± SEM (n = 10–12 per group). *$p < 0.05$; **$p < 0.01$; ***$p < 0.001$ vs. the vehicle-treated EAE mice

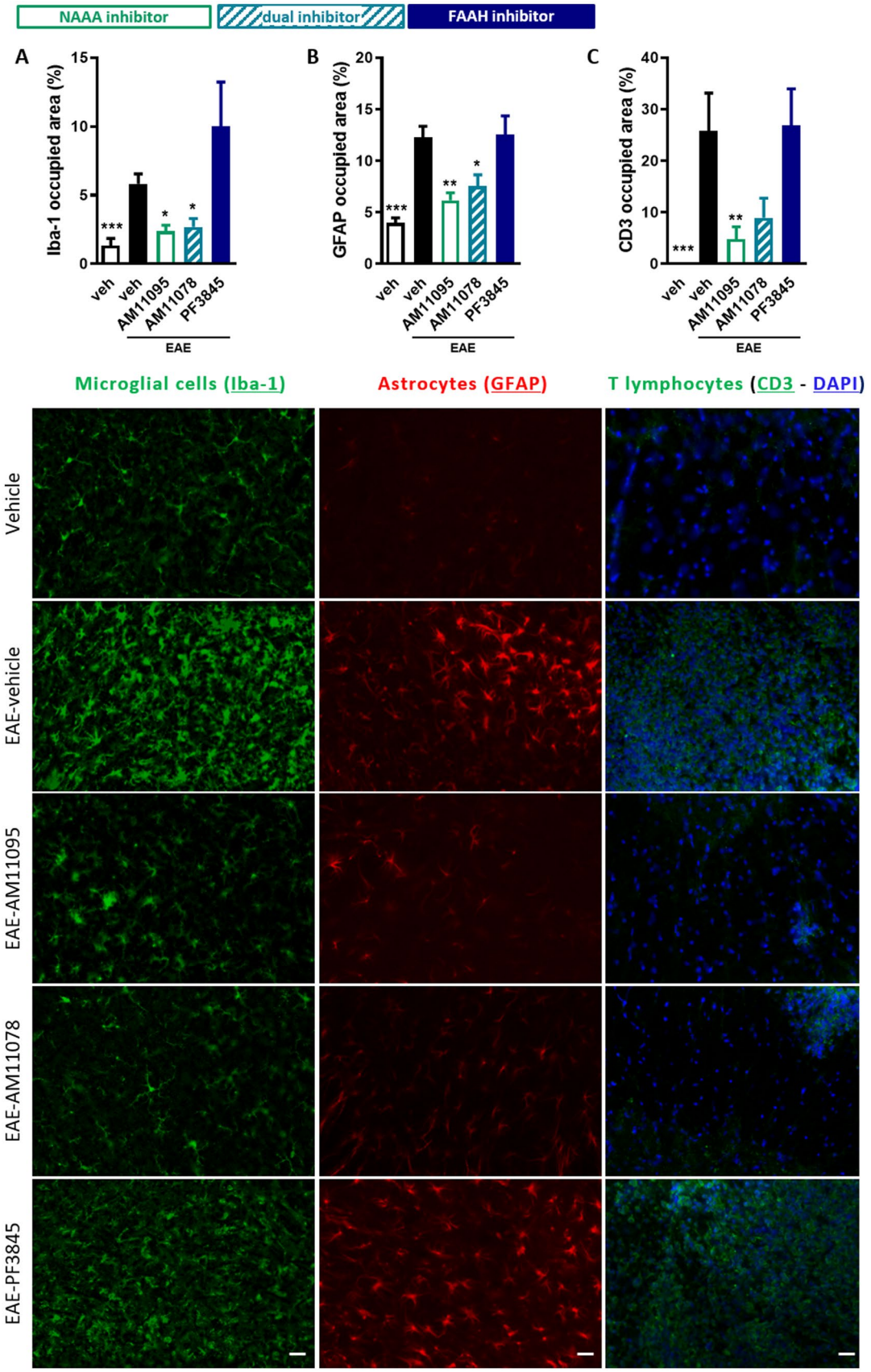


B

NAAA inhibitor | dual inhibitor | FAAH inhibitor

Group	Disease incidence	Mean of maximum score	Median of maximum score	Mean day of onset	AUC
EAE-vehicle	11/12	2.77 ± 0.38	4.0	12.55 ± 0.34	39.41 ± 6.15
EAE-AM11095	5/12	1.17 ± 0.38 **	0.5	15.60 ± 1.12 *	9.81 ± 3.90 **
EAE-AM11078	7/12	1.44 ± 0.37*	1.25	13.17 ± 0.79	14.89 ± 4.22 *
EAE-PF3845	9/12	2.56 ± 0.42	3.75	13.27 ± 0.45	33.19 ± 6.93

Fig. 2 NAAA inhibition decreased EAE progression and delayed the onset of the symptoms. EAE was induced in C57BL/6J female mice by immunization with $MOG_{35–55}$ in CFA on day 0 and PTX injections on days 0 and 1. The NAAA inhibitor, AM11095 (15 mg/kg, b.i.d.), the dual NAAA-FAAH inhibitor, AM11078 (15 mg/kg, b.i.d.), the FAAH inhibitor, PF-3845 (10 mg/kg, q.d.), or vehicle (veh) were administered intraperitoneally, starting from day 3 after EAE induction (represented by the arrow) to day 30. Control (CTL) mice received CFA emulsion on day 0 and vehicle of PTX on days 0 and 1. Mice were killed on day 30 post immunization. **(A)** EAE clinical score progression. **(B)** Disease incidence (characterized by a limp tail), mean and median of maximum clinical score during the first phase of the disease (from day 13 to day 22 post immunization), mean day of onset as well as mean AUC values for the clinical score are summarized in the table. Except for the mean day of onset, all parameters were calculated on all mice. Data represent mean ± SEM (n = 10–12 per group). *$p < 0.05$; **$p < 0.01$ vs. vehicle-treated EAE mice


NAAA inhibitor
dual inhibitor
FAAH inhibitor
A
Iba-1 occupied area (%)
B
GFAP occupied area (%)
C
CD3 occupied area (%)
veh
veh
AM11095
AM11078
PF3845
EAE
Microglial cells (Iba-1)
Astrocytes (GFAP)
T lymphocytes (CD3 - DAPI)
Vehicle
EAE-vehicle
EAE-AM11095
EAE-AM11078
EAE-PF3845

show clinical signs, on average, 3 days after the vehicle-treated EAE mice. The mean maximal score reached, at the peak of disease, by all the mice treated with AM11095 was lower than the vehicle-treated mice (Fig. 2A, B). When considering only the mice that developed the disease, AM11095 treatment did not significantly decrease this score (2.3 ± 0.6) compared to the score reached by vehicle-treated EAE mice (3.0 ± 0.3). Although 3 mice treated with the FAAH inhibitor PF-3845 did not develop the disease, overall PF-3845 administration had no significant beneficial effect on the severity of the disease, the day of the onset and the maximum clinical score reached by the mice (Fig. 2A, B). The dual FAAH and NAAA inhibitor AM11078 reduced EAE progression in a similar manner to AM11095 (Fig. 2A, B). When receiving AM11078, 5 mice out of 12 remained free of disease. Although the treatment did not delay the onset of clinical signs, it reduced the severity of the disease (Fig. 2A, B). The effect of AM11078 was statistically significant even if considering only the mice that developed the disease (2.1 ± 0.5 vs. 3.0 ± 0.3).

NAAA Inhibition and Dual NAAA-FAAH Inhibition, but Not FAAH Inhibition, Lowered Glial Cell Activation and Lymphocyte Infiltration in the Spinal Cord of EAE Mice

MS and EAE inflammatory events and lesions are due to the activation of resident microglia and astrocytes as well as to the infiltration of lymphocytes [40]. Thus, at the end of the experiment, we evaluated glial cell (microglia and astrocytes) activation and T lymphocyte infiltration in the spinal cord of these mice.

In the vehicle-treated EAE mice, we found an increase in the areas occupied by Iba-1-positive (microglia) (Fig. 3A), GFAP-positive (astrocytes) (Fig. 3B), and CD3-positive (lymphocytes) cells (Fig. 3C) compared to the control group. In the spinal cord of mice treated with the NAAA inhibitor or the dual NAAA-FAAH inhibitor, we observed a decrease in GFAP and Iba-1 staining. A decrease in T lymphocyte infiltration, evidenced by decreased CD3-positive cells, was only observed for EAE mice treated with the NAAA inhibitor. Interestingly, no difference was observed for these parameters when mice were treated with the FAAH inhibitor (Fig. 3A–C).

NAAA Inhibition Protected from Spinal Cord Demyelination and Reduced Inflammation Contrary to FAAH Inhibition or Dual NAAA-FAAH Inhibition

Demyelination was assessed by measuring the percentage of LFB-unstained area in the spinal cord white matter. Vehicle-treated EAE mice showed a greater LFB-unstained area, indicative of myelin loss when compared to the control group (Fig. 4A, B). NAAA inhibition reduced the LFB-unstained area compared to the vehicle-treated EAE mice. However, no difference in the extent of demyelination was observed between mice treated with either the FAAH inhibitor or with the dual NAAA-FAAH inhibitor compared to vehicle-treated EAE mice (Fig. 4A, B).

Next we compared the effects of NAAA inhibition, of FAAH inhibition, or of the dual NAAA-FAAH inhibition on the expression of inflammatory markers in the spinal cord of the mice. Compared to control mice, $MOG_{35–55}$ immunization

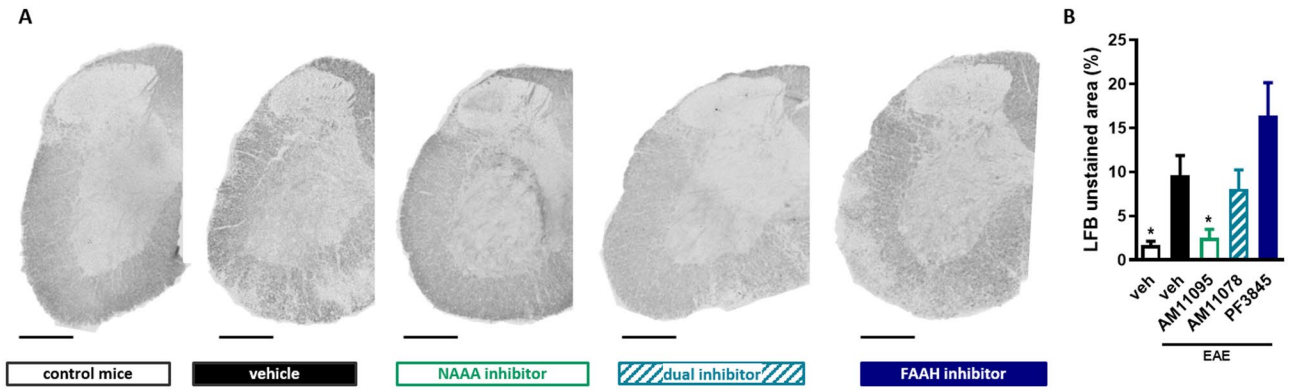


Fig. 4 NAAA inhibition decreased spinal cord demyelination in EAE mice. EAE was induced in C57BL/6J female mice by immunization with $MOG_{35–55}$ in CFA on day 0 and PTX injections on days 0 and 1. The NAAA inhibitor, AM11095 (15 mg/kg, b.i.d.), the dual NAAA-FAAH inhibitor, AM11078 (15 mg/kg, b.i.d.), the FAAH inhibitor, PF-3845 (10 mg/kg, q.d.), or vehicle (veh) were administered intraperitoneally, starting from day 3 after EAE induction to day 30. Control (CTL) mice received CFA emulsion on day 0 and vehicle of PTX on days 0 and 1. Mice were killed on day 30 post immunization. **(A)** Representative photomicrographs and **(B)** quantification of luxol fast blue (LFB)-unstained area in the ventral white matter of the spinal cord (i.e., (LFB-unstained area of the ventral white matter / total area of the ventral white matter) × 100). The scale bar represents 200 µm. Data are reported as mean ± SEM (n = 10–12 per group). *$p < 0.05$ vs. the vehicle-treated EAE mice

increased mRNA expressions of IFNγ, IL-1β, TNF-α, and MIP1α (Fig. 5A), and protein production of RANTES, MIP1α, and IL-12 (Fig. 5B). We also observed a trend to increase for IL-1 β and G-CSF (Fig. 5B). mRNA expression of activating transcription factor 3 (ATF3), a sensitive marker of damaged sensory neurons [41], was also increased in vehicle-treated EAE mice compared to control mice (Fig. 5A). Interestingly, in the spinal cord, IL-6 and KC protein levels were not altered by the pathology (Fig. 5B). Administration of the NAAA inhibitor AM11095 resulted in the reduction of all the markers that were increased by the disease (Fig. 5A, B). In contrast, the administration of the FAAH or the dual NAAA-FAAH inhibitor, although sometimes exhibiting a trend toward a reduction in these inflammatory parameters, did not reach statistical significance.

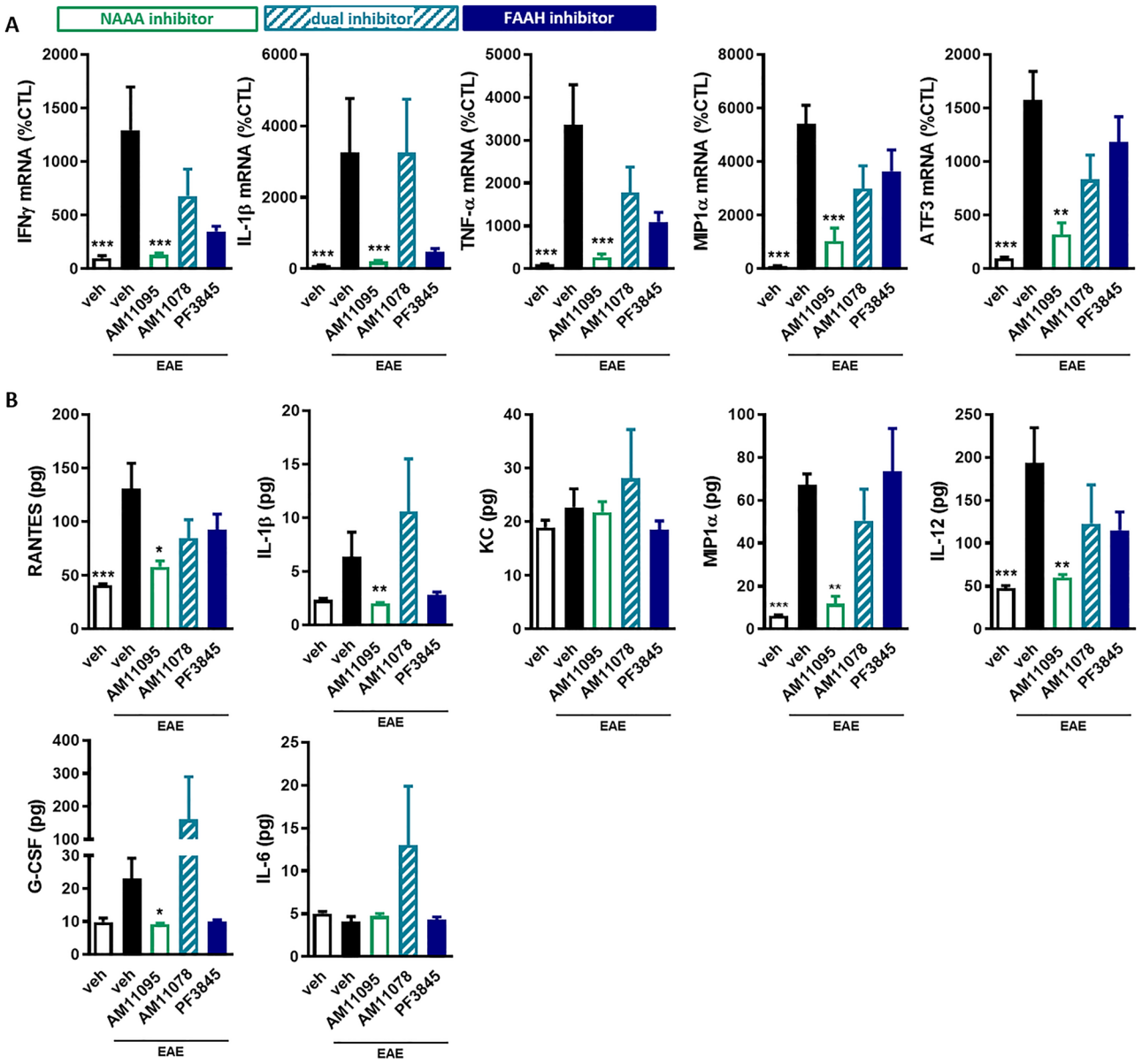


Fig. 5 NAAA inhibition decreased inflammatory markers in the spinal cord of EAE mice. EAE was induced in C57BL/6J female mice by immunization with $MOG_{35–55}$ in CFA on day 0 and PTX injections on days 0 and 1. The NAAA inhibitor, AM11095 (15 mg/kg, b.i.d.), the dual NAAA-FAAH inhibitor, AM11078 (15 mg/kg, b.i.d.), the FAAH inhibitor, PF-3845 (10 mg/kg, q.d.), or vehicle (veh) were administered intraperitoneally, starting from day 3 after EAE induction to day 30. Control (CTL) mice received CFA emulsion on day 0 and vehicle of PTX on days 0 and 1. Mice were killed on day 30 post immunization. (**A**) mRNA expressions of inflammatory markers were measured in the spinal cord by RT-qPCR with RPL19 used as a reference. Data are expressed as percentage of the control group. (**B**) Cytokine production was assessed by multiplex ELISA in the spinal cord and expressed as pg/45 µg of proteins. Data represent mean ± SEM (n = 10–12 per group). $*p < 0.05$; $**p < 0.01$; $***p < 0.001$ vs. the vehicle-treated EAE mice

Mice Receiving the NAAA Inhibitor or a Co-administration of the NAAA Inhibitor and the FAAH Inhibitor, Starting 11 Days Post Immunization, Showed Reduced Clinical and Histopathological Features of EAE

When administered prophylactically (i.e., 3 days post $MOG_{35–55}$), AM11095 administration delayed the onset of the disease and decreased inflammatory hallmarks in the spinal cord. To establish compound efficacy after disease onset, we repeated the study but administered the inhibitors at symptoms onset (i.e., 11 days after immunization). At this point, 25% of the mice had at least a limped tail tip as clinical sign. In this study, we also compared the effects of the dual NAAA-FAAH inhibitor (AM11078) to the effects of the co-administration of the NAAA (AM11095) and FAAH (PF-3845) inhibitors.

NAAA Inhibition Reduced EAE-Associated Clinical Score

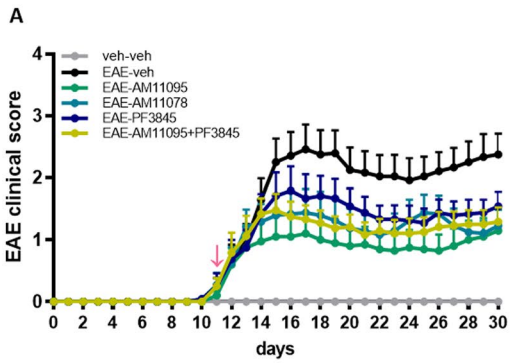
Mice receiving AM11095 displayed a less severe course of the disease as displayed by a decreased cumulative clinical score (for the whole cohort) measured by the area under the curve and a lower maximal score (Fig. 6). This observation could be explained, at least in part, by a protective effect of the NAAA inhibitor against EAE pathogenesis. Indeed, even though the treatment was given later in the progression of the disease (compared to the previous study) 4 mice out of 12 remained free of disease while all the vehicle-treated EAE mice (i.e., 12/12) exhibited clinical signs of the disease. Again, when the maximal score was calculated for sick mice only, even though a trend toward a decrease was observed, the difference between mice treated with AM11095 and vehicle did not reach significance (2.2 ± 0.4 vs. 2.7 ± 0.4).

Similarly to the first study, the administration of the FAAH inhibitor PF-3845 did not result in a statistically significant effect on disease evolution (Fig. 6). Interestingly, the administration of the dual inhibitor AM11078 and the co-administration of AM11095 and PF-3845 resulted in a similar improvement of the disease course when compared to vehicle-treated mice (Fig. 6). Actually the three groups of mice that received a NAAA inhibitor had an improvement of their disease course as evidenced by a reduction of the maximum score reached and of the AUC of the clinical score evolution.

NAAA Inhibition and Dual NAAA-FAAH Inhibition Lowered Microglia Activation and Lymphocyte Infiltration in the Spinal Cord of EAE Mice

Consistent with the EAE model [40], the percentage of areas occupied by Iba-1-positive (microglia), GFAP-positive (astrocytes), and CD3-positive (lymphocytes) cells were increased in the spinal cord white matter of vehicle-treated EAE mice compared to the control group (Fig. 7A–C).

A decrease in microglia activation, evidenced by a decrease in Iba-1 staining, was observed in the spinal cord of EAE mice treated with the NAAA inhibitor, the dual inhibitor, and the mixture of the NAAA and FAAH inhibitors (Fig. 7A). Contrary to the first study, none of the treatments resulted in a decrease in GFAP positive area (Fig. 7B), while CD3 staining was decreased in the inhibitor-treated groups compared to vehicle-treated EAE mice (Fig. 7C).



B

Group	Disease incidence	Mean of maximum score	Median of maximum score	AUC
EAE-vehicle	12/12	2.69 ± 0.37	3.125	37.69 ± 6.03
EAE-AM11095	8/12	1.35 ± 0.41*	1.50	17.28 ± 5.13**
EAE-AM11078	11/12	1.79 ± 0.34*	1.75	23.20 ± 5.24*
EAE-AM11095 and PF3845	10/12	1.77 ± 0.26*	2.0	22.52 ± 3.99*
EAE-PF3845	10/12	2.12 ± 0.38	2.5	26.50 ± 4.71

NAAA inhibitor | dual inhibitor | NAAA inhibitor + FAAH inhibitor | FAAH inhibitor

Fig. 6 NAAA inhibition and the concomitant inhibition of NAAA and FAAH, from the onset of the disease, decreased EAE severity. EAE was induced in C57BL/6J female mice by immunization with $MOG_{35–55}$ in CFA on day 0 and PTX injections on days 0 and 1. The NAAA inhibitor, AM11095 (15 mg/kg, b.i.d.), the dual NAAA-FAAH inhibitor, AM11078 (15 mg/kg, b.i.d.), the FAAH inhibitor, PF-3845 (10 mg/kg, q.d.), a combination of AM11095 (15 mg/kg, b.i.d.) with PF-3845 (10 mg/kg, q.d.), or vehicle (veh) were administered intraperitoneally, starting from the onset of the disease (day 11) (represented by the arrow) to day 30. Control (CTL) mice received CFA emulsion on day 0 and vehicle of PTX on days 0 and 1. Mice were killed on day 30 post immunization. **(A)** EAE clinical score progression. **(B)** Disease incidence (characterized by a limp tail), mean and median of maximum clinical score during the first phase of the disease (from day 13 to day 22 post immunization) as well as mean AUC values for the clinical score (EAE score) are summarized in the table. All parameters were calculated on all mice. Data represent mean ± SEM (n = 10–12 per group). *$p < 0.05$; **$p < 0.01$ vs. the vehicle-treated EAE mice

Treatment with the NAAA Inhibitor or the Combination of NAAA and FAAH Inhibitors Protected from Spinal Cord Demyelination and Reduced Inflammatory Markers in EAE Mice

Vehicle-treated EAE mice presented a demyelination in the spinal cord white matter evidenced by a larger Fluoromyelin Green–unstained area compared to the control group (Fig. 7D). This unstained area was significantly reduced in mice treated with AM11095 (either alone or in combination with PF-3845) (Fig. 7D). The FAAH inhibitor when administered alone had less effect on this parameter.

As in the previous study, the spinal cord of vehicle-treated EAE mice is characterized by an increase in disease markers mRNA expression (IFNγ, IL-1β, TNF-α, MIP1α, and ATF3) (Fig. 8A) and protein production (RANTES, IL-1β, KC, MIP1α, and IL-6) (Fig. 8B). As for the demyelination, treatment with the NAAA inhibitor AM11095, either alone or in combination with the FAAH inhibitor PF-3845, decreased most of the markers studied (Fig. 8A, B). Overall, administration of the FAAH inhibitor alone and of AM11078 (the dual inhibitor) was less efficient in counteracting spinal cord inflammation.

Differential Regulation of NAE Levels Following NAAA, FAAH, or Dual NAAA-FAAH Inhibition in the Central Nervous System and the Plasma

To dissect the differences between the effects of NAAA, FAAH, and the dual NAAA-FAAH inhibition in EAE mice, we measured the levels of NAEs (i.e., AEA, PEA, OEA, and SEA) in the spinal cord, the brain, and the plasma.

In these three tissues, we did not find any statistically significant difference in NAE levels between control and vehicle-treated EAE mice. The levels of AEA, OEA, PEA, and SEA were increased following FAAH inhibition with PF-3845 in the CNS and plasma (Fig. 9A–C). However, no increase was detected for the EAE mice treated with the NAAA inhibitor AM11095 compared to the vehicle-treated EAE mice (Fig. 9A–C). On the other hand, AM11078 increased NAE levels although to a lower extent than PF-3845 (Fig. 9A–C).

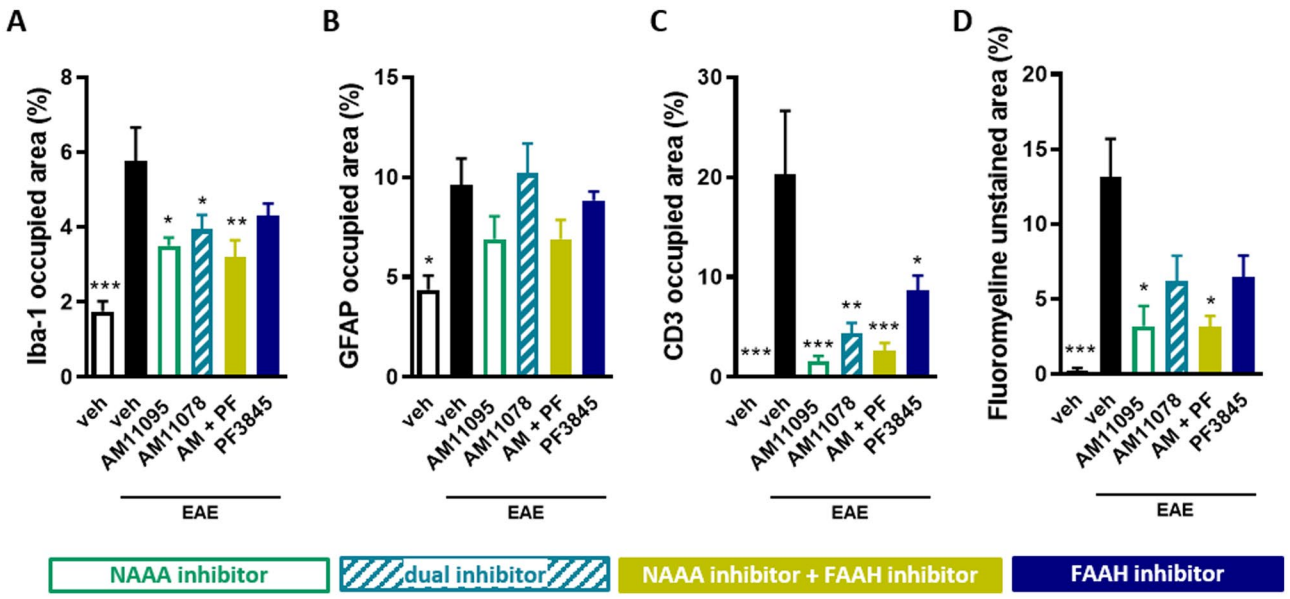


Fig. 7 NAAA inhibition and concomitant NAAA and FAAH inhibition, from the onset of the disease, reduced demyelination, glial cell activation and lymphocyte presence in the spinal cord of mice. EAE was induced in C57BL/6J female mice by immunization with $MOG_{35–55}$ in CFA on day 0 and PTX injections on days 0 and 1. The NAAA inhibitor, AM11095 (15 mg/kg, b.i.d.), the dual NAAA-FAAH inhibitor, AM11078 (15 mg/kg, b.i.d.), the FAAH inhibitor, PF-3845 (10 mg/kg, q.d.), a combination of AM11095 (15 mg/kg, b.i.d.) with PF-3845 (10 mg/kg, q.d.), (AM + PF), or vehicle (veh) were administered intraperitoneally, starting from the onset of the disease (day 11) to day 30. Control (CTL) mice received CFA emulsion on day 0 and vehicle of PTX on days 0 and 1. Mice were killed on day 30 post immunization. The area occupied in the spinal cord by (**A**) Iba-1 positive cells (microglia), (**B**) GFAP positive cells (astrocytes), and (**C**) CD3 positive cells (T lymphocytes) was quantified and expressed as percentage (i.e., (marker-positive area of the ventral white matter / total area of the ventral white matter) × 100). (**D**) Quantification of Fluoromyelin Green unstained area in the ventral white matter of the spinal cord expressed as percentage (i.e., (Fluoromyelin Green-unstained area of the ventral white matter / total area of the ventral white matter) × 100). Data are reported as mean ± SEM (n = 8–9 per group). *$p < 0.05$; **$p < 0.01$; ***$p < 0.001$ vs. the vehicle-treated EAE mice

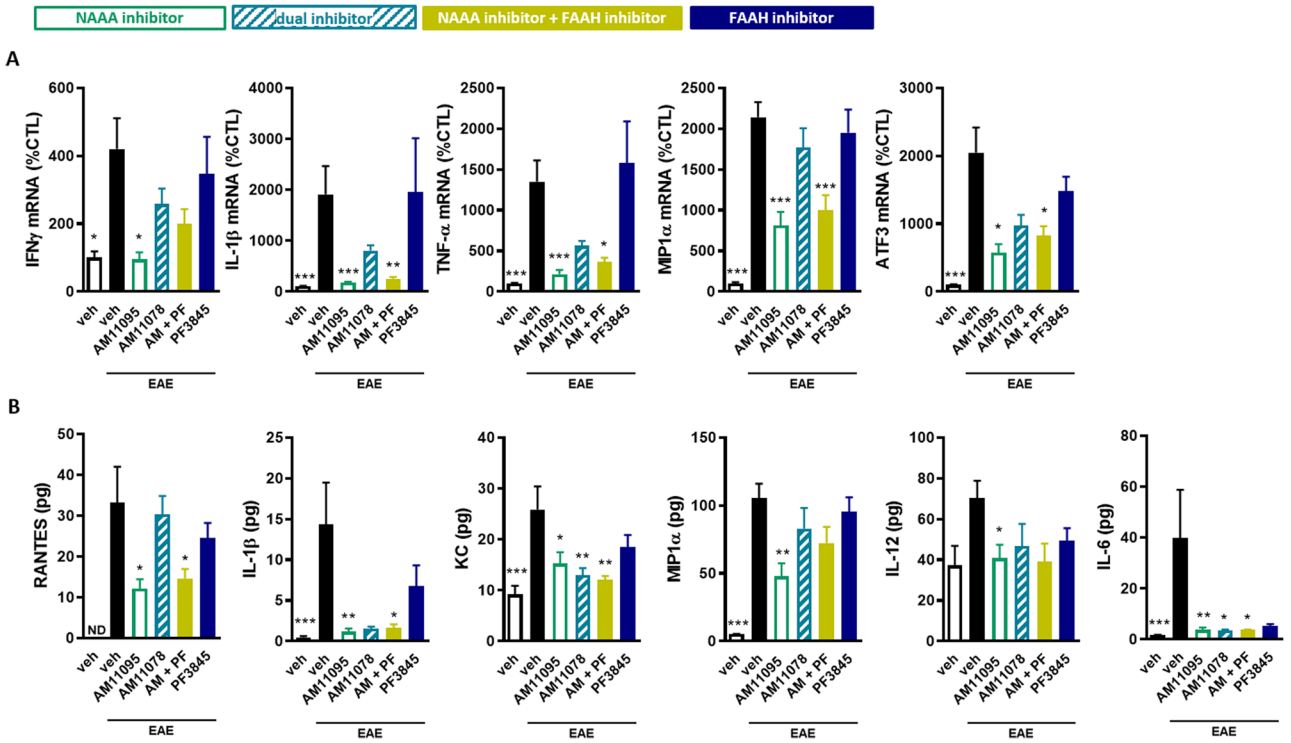


Fig. 8 NAAA inhibition and concomitant NAAA and FAAH inhibition, from the onset of the disease, decreased inflammatory markers in the spinal cord of EAE mice. EAE was induced in C57BL/6J female mice by immunization with $MOG_{35–55}$ in CFA on day 0 and PTX injections on days 0 and 1. The NAAA inhibitor, AM11095 (15 mg/kg, b.i.d.), the dual NAAA-FAAH inhibitor, AM11078 (15 mg/kg, b.i.d.), the FAAH inhibitor, PF-3845 (10 mg/kg, q.d.), a combination of AM11095 (15 mg/kg, b.i.d.) with PF-3845 (10 mg/kg, q.d.) (AM + PF), or vehicle (veh) were administered intraperitoneally, starting from the onset of the disease (day 11) to day 30. Control (CTL) mice received CFA emulsion on day 0 and vehicle of PTX on days 0 and 1. Mice were killed on day 30 post immunization. (**A**) mRNA expressions of inflammatory markers were measured in the spinal cord by RT-qPCR with RPL19 used as a reference gene. Data are expressed as percentage of the control group. (**B**) Cytokine production was assessed by multiplex assay (U-PLEX) in the spinal cord and expressed as pg/45 µg of proteins. Data represent mean ± SEM (n = 10–12 per group). $*p < 0.05$; $**p < 0.01$; $***p < 0.001$ vs. vehicle-treated EAE mice

NAAA Inhibition, FAAH Inhibition, and Dual NAAA-FAAH Inhibition Increased NAE Levels and Decreased the Expression of Pro-inflammatory Markers in a Primary Co-culture of Astrocytes and Microglia

As mentioned, astrocytes and microglia are important players in the inflammatory response of the CNS and play a crucial role in MS [1]. Using a primary co-culture of mouse astrocytes and microglia, we showed that both NAAA and FAAH were expressed in these cells, although when comparing the ΔCt for both enzymes, NAAA was far more expressed than FAAH (Fig. S1B).

Therefore, we sought to assess the effects of these inhibitors in this primary co-culture. Interestingly, all inhibitors increased NAE levels and showed globally the same magnitude in their effect when looking at AEA, PEA, OEA, and SEA levels (Fig. 10A). Of note, we did not observe any additional effect when NAAA and FAAH were blocked simultaneously using the dual inhibitor (Fig. 10A). Interestingly, the inhibitors had similar effects when incubated with co-culture activated with IFNγ and TNF-α, two inflammatory cytokines contributing to the pathogenesis of EAE [42] (Fig. 10B). Although we did not find any variation in NAE levels in the tissues of the CNS, these data support the efficacy of AM11095 and AM11078 in increasing NAE levels in these important glial cells in the context of MS.

We also assessed the effects of the three inhibitors on the activation of this primary culture by IFNγ and TNF-α. Incubation of the cells with the two cytokines resulted in increased mRNA expression of iNOS, TNF-α, IL-6, MIP1α, and IL-1β as well as increased production of IL-6 (Fig. S2A). The NAAA inhibitor AM11095 and the dual NAAA-FAAH inhibitor AM11078 were able to decrease most of the inflammatory markers increased by IFNγ and TNF-α (Fig. 10C). Despite a

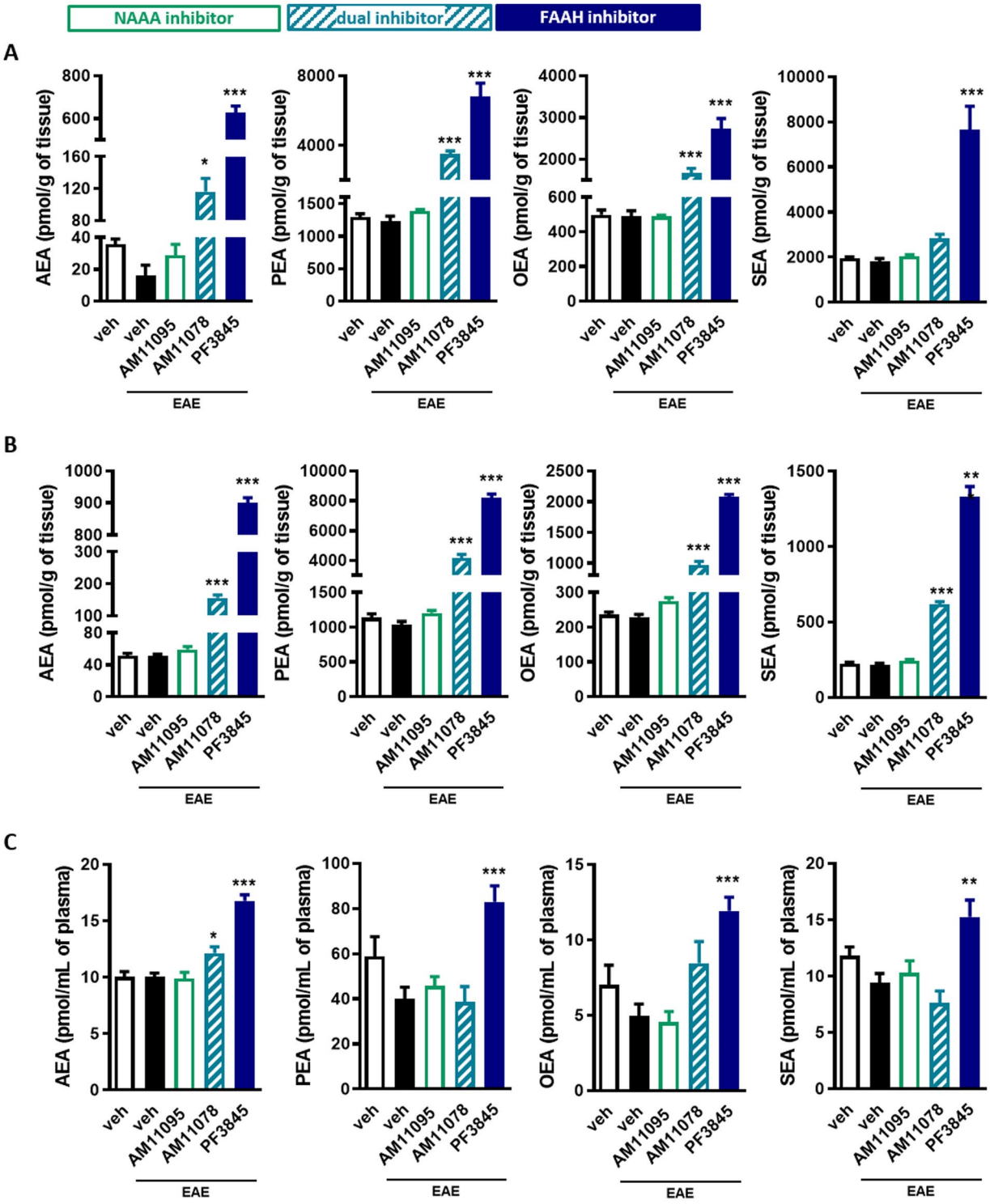


Fig. 9 Alteration of *N*-acylethanolamine levels in the spinal cord, the brain, and the plasma of EAE mice following enzyme inhibition. EAE was induced in C57BL/6J female mice by immunization with $MOG_{35–55}$ in CFA on day 0 and PTX injections on days 0 and 1. The NAAA inhibitor, AM11095 (15 mg/kg, b.i.d.), the dual NAAA-FAAH inhibitor, AM11078 (15 mg/kg, b.i.d.), the FAAH inhibitor, PF-3845 (10 mg/kg, q.d.), or vehicle (veh) were administered intraperitoneally, starting from day 3 after EAE induction to day 30. Mice were killed on day 30 post immunization. *N*-acylethanolamine (AEA, PEA, OEA, and SEA) levels were measured by UPLC-MS/MS in (**A**) the spinal cord, (**B**) the brain, and (**C**) plasma of EAE mice. For (**A**) and (**B**), data are expressed as pmol per g of tissue, and for (**C**) as pmol per mL of plasma. Data represent mean ± SEM (n = 10–12 per group). $^{*}p < 0.05$; $^{**}p < 0.01$; $^{***}p < 0.001$ vs. the vehicle-treated EAE mice

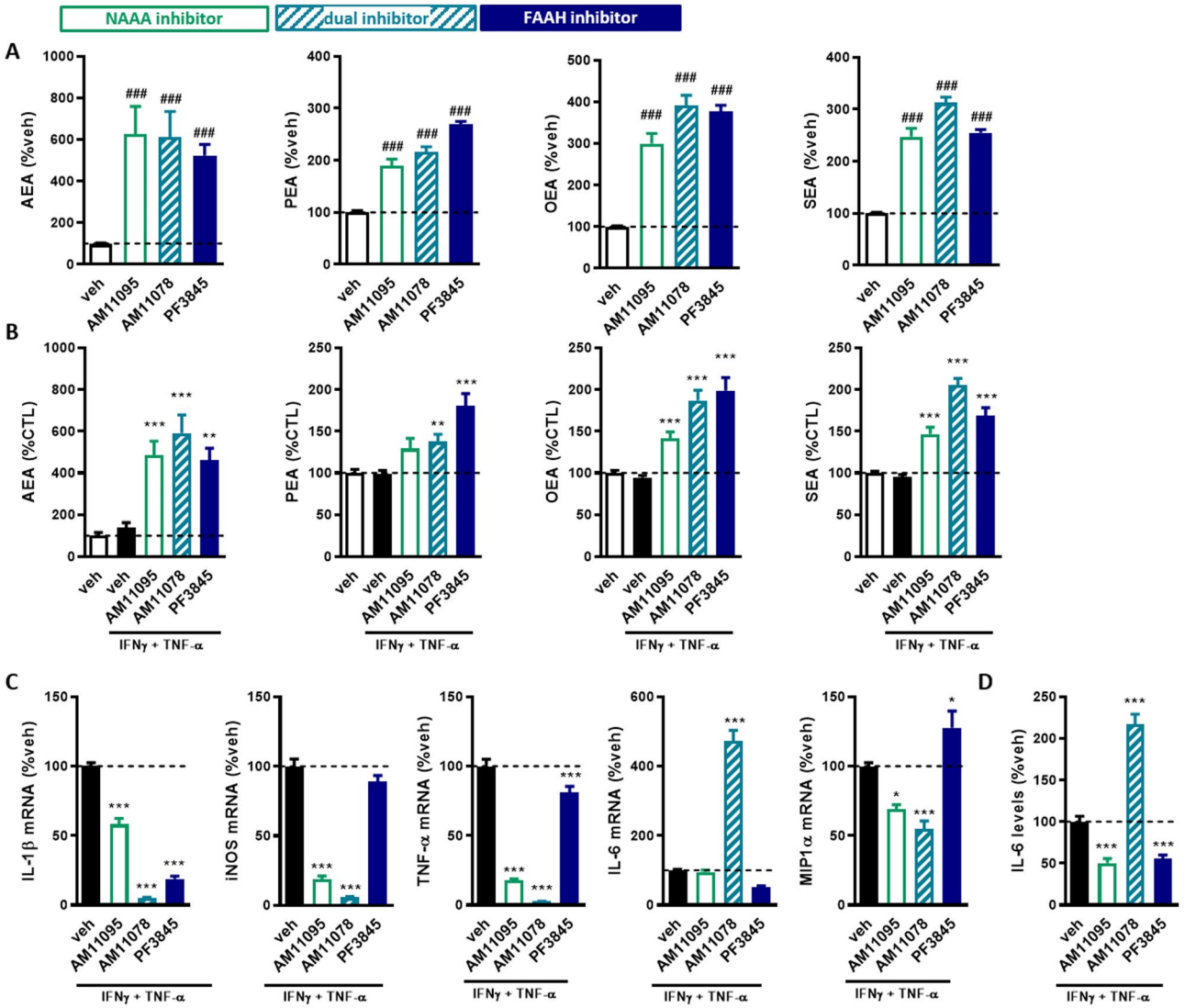


Fig. 10 NAAA inhibition and dual NAAA-FAAH inhibition increased *N*-acylethanolamine levels and decreased cytokine expression in primary co-culture of astrocytes and microglia. (**A**, **B**) *N*-acylethanolamine levels measured by UPLC-MS/MS following incubation of the primary co-culture with either NAAA, FAAH, or dual NAAA-FAAH inhibitors (10 µM) or DMSO vehicle (DMSO 0.1%). (**A**) Cells were incubated with vehicle, AM11095, AM11078, or PF-3845 for 6 h or (**B**) pre-incubated with vehicle or the enzyme inhibitors for 1 h before stimulation with IFNγ (20 ng/mL) and TNF-α (50 ng/mL) for 5 h. Results are expressed as percentage of the NAE levels in the control condition represented by the dotted line. Data represent mean ± SEM from 3 separate experiments (measurements in triplicates). (**C**, **D**) Primary co-cultures of astrocytes and microglia were pre-incubated with vehicle (veh, DMSO 0.1%) or the enzyme inhibitors (10 µM) for 1 h before stimulation with IFNγ (20 ng/mL) and TNF-α (50 ng/mL) for 8 h. (**C**) mRNA expressions of inflammatory markers were measured by RT-qPCR with RPL19 used as a reference gene. (**D**) IL-6 production was assessed by ELISA in the culture medium. Data represent mean ± SEM from 3 separate experiments (measurements in triplicates) and are expressed in percentage of the IFNγ and TNF-α-untreated group (veh). $^{###}p < 0.001$ vs. the control group and $^{*}p < 0.05$; $^{**}p < 0.01$; $^{***}p < 0.001$ vs. the IFNγ and TNF-α-untreated group

similar increase in NAE levels as the other inhibitors, FAAH inhibition using PF-3845 had quite different effects when compared to AM11095 (Fig. 10C).

Considering that LPS is often used in the literature to activate immune cells in the context of neuroinflammation (e.g., refs. [43, 44]), we sought to assess the effect of AM11095, AM11078, and PF-3845 on LPS-activated primary co-culture of astrocytes and microglia (Fig. S2B). Generally, the same effects of AM11095 and AM11078 were observed on NAE levels (Fig. S3A) and on pro-inflammatory mediator mRNA expression and production when cells were activated with LPS or the combination of IFNγ and TNF-α (Fig. S3B). Of note, PF-3845 was less efficient in decreasing cell activation by LPS (Fig. S3B).

Effects of the NAAA and/or FAAH Inhibition on Systemic Immune Response

Another potential mechanism of action of drugs in the context of MS is to act on the peripheral immune response [45]. To assess the effect of the inhibitors on lymphocyte response to MOG immunization, mice were immunized with $MOG_{35–55}$ and treated with the inhibitors as in the previous experiments. On day 14, we performed ex vivo a T cell recall experiment using $MOG_{35–55}$. Following ex vivo antigen-activation of spleen cells from immunized mice, the mRNA expressions of the pro-inflammatory cytokines IFNγ and TNF-α, two major cytokines of the Th1 response, and IL-17 and IL-22, implicated in the Th17 response [46], was increased. The expression of FOXP3, an important transcription factor for Treg response [46], was increased as well, although IL-10 mRNA expression was not increased (Fig. 11A). Treatment of the mice with the inhibitors did not decrease the expressions of the different Th1/Th17 markers accompanying EAE after T cell recall [46]. Additionally, Treg response-associated markers were decreased in cells recovered from lymph nodes of NAAA inhibitor-treated EAE mice following MOG restimulation (Fig. 11B). These observations suggest that the beneficial effects of NAAA inhibition on EAE pathogenesis are independent of a decrease in T cell activation.

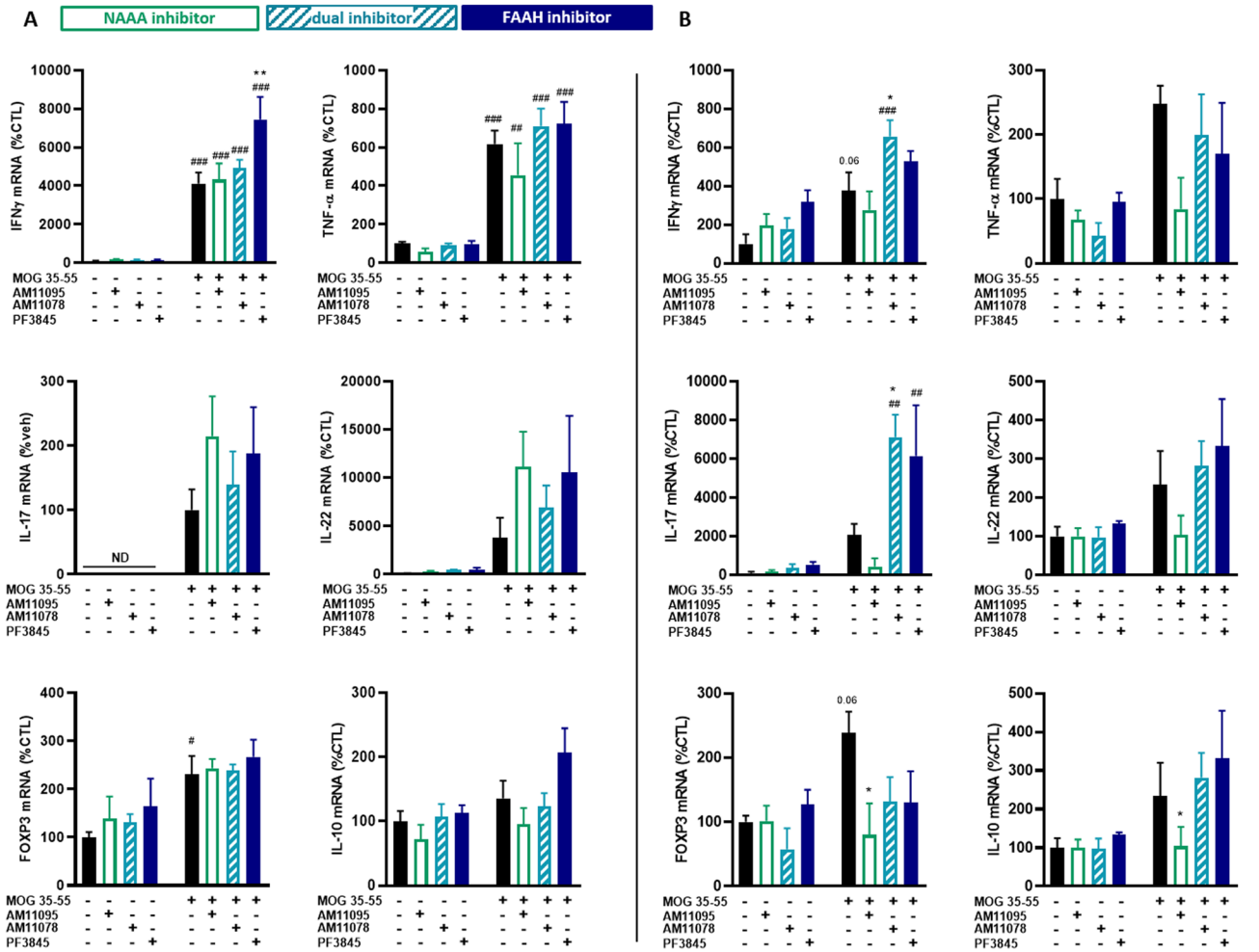


Fig. 11 NAAA and FAAH inhibition did not decrease Th1/Th17 peripheral immune response following MOG immunization in EAE mice. EAE was induced in C57BL/6J female mice by immunization with $MOG_{35–55}$ in CFA on day 0 and PTX injections on days 0 and 1. The NAAA inhibitor, AM11095 (15 mg/kg, b.i.d.), the dual NAAA-FAAH inhibitor, AM11078 (15 mg/kg, b.i.d.), the FAAH inhibitor, PF-3845 (10 mg/kg, q.d.), or vehicle (veh) were administered intraperitoneally, starting from day 3 to day 14. On day 14 post immunization, leukocytes recovered from **(A)** the spleen and **(B)** lymph nodes were restimulated in vitro with $MOG_{35–55}$ (20 µg/mL) for 48 h. mRNA expressions of IFNγ, TNF-α, IL-17, IL-22, IL-10, and FOXP3 were measured by RT-qPCR with RPL19 used as a reference gene. Data represent mean ± SEM and are expressed as % of MOG-unstimulated cells recovered from the vehicle-treated EAE mice (n = 4 mice per group). In (**A**), IL-17 mRNA expression was detectable only following splenocyte recall with the MOG antigen and the data are expression as % of the MOG-restimulated splenocytes recovered from vehicle-treated EAE mice. ND is for not detectable. Data were analyzed with a two-way ANOVA. $^{\#}p < 0.05$; $^{\#\#}p < 0.01$; $^{\#\#\#}p < 0.001$ is indicative of a difference following $MOG_{35–55}$ T cell recall and $^{*}p < 0.05$; $^{**}p < 0.01$ is indicative of an effect of the inhibitors

Effects of *N*-Acyltaurines and *N*-Acylglycines in Primary Co-culture of Astrocytes and Microglia

Besides NAEs, other fatty acyl amides such as *N*-acyltaurines or *N*-acylglycines have been described as substrates for FAAH [47–49]. Indeed, *N*-acyltaurines and *N*-acylglycines were shown to be increased following chronic FAAH inhibition or FAAH deletion [47–51]. If these FAAH substrates exert deleterious effects, then their increase following FAAH inhibition could potentially explain the differences between FAAH and NAAA inhibitions on inflammatory parameters. Therefore, we tested on a primary co-culture of mouse astrocytes and microglia different species of these two families of long-chain *N*-acylamines. Incubation of the cells with 18:1 *N*-acyltaurine, 20:0 *N*-acyltaurine, and 20:4 *N*-acyltaurine increased IL-1β mRNA expression (Fig. S4A). Moreover, 20:0 *N*-acyltaurine also increased TNF-α mRNA expression and IL-6 protein production (Fig. S4A, B). 20:4 *N*-acylglycine also increased IL-1β and TNF-α mRNA expressions and IL-6 production (Fig. S4C, D). IL-6 protein production in the media was also increased following incubation with 16:0 *N*-acylglycine (Fig. S4D).

Discussion

In this study, we compared in the same settings the effects of NAAA inhibition, FAAH inhibition, and dual NAAA-FAAH inhibition in the murine EAE model of MS. NAEs are reported to exert beneficial effects in the context of inflammation and neuroprotection [7, 12, 52]. Therefore, blocking their hydrolysis seemed a promising strategy to increase NAE endogenous levels and counteract the progression and the severity of EAE.

Although both NAAA and FAAH hydrolyze NAEs, we showed here, by comparing their inhibition in similar set ups, that NAAA seems to be a more attractive target in the context of MS. Indeed its inhibition delayed the onset of the disease and reduced its severity while, in our hands, inhibiting FAAH did not produce the same beneficial effects as NAAA inhibition. We also found that the FAAH inhibitor PF-3845 does not seem to exert the same effects on EAE mice when the treatment is initiated 3 days post immunization or 11 days post immunization (at disease onset). Indeed, a later FAAH inhibition appears to induce a trend toward a decrease of different features of the pathology. The difference observed between the two treatment schemes could potentially be explained by the different pool of cells present (or their activation status) at the beginning of PF-3845 administration. In fact, the discrepancies observed with FAAH inhibition according to the experimental settings could potentially explain the discordant effects of URB597 and FAAH deletion in multiple sclerosis models encountered in the literature [22–24].

Our investigations on the potential mechanisms by which the NAAA inhibitor AM11095 attenuates EAE severity suggest that the effects of NAAA inhibition could be, at least in part, attributable to its ability to decrease inflammatory mediator expression in astrocytes and microglia and not by altering immune response from the periphery. Indeed, when using splenocytes and draining lymph node cells isolated from EAE mice treated with either vehicle or with AM11095, we did not observe a decrease in cytokine expression by T cells upon MOG stimulation. Conversely, the inhibitor reduced the activation of primary glial cells. These observations in vitro are reinforced by the reduced expressions of Iba-1 and GFAP found in the spinal cord of EAE mice following NAAA inhibition. The administration of a NAAA inhibitor in EAE mice could therefore interfere positively with the course of the disease by blocking the activation of immune resident cells and decreasing neuroinflammation, infiltration of immune cells in the CNS, and demyelination.

Interestingly, the beneficial effects we observed when the NAAA inhibitor AM11095 was administered at the beginning of the study (i.e., 3 days post immunization) were also present when AM11095 was administered at the onset of the first clinical sign.

Another interesting observation is that despite NAE levels being increased with either of the three inhibitors in the primary co-culture of astrocytes and microglia, we were not able to show any significant increase in NAE levels in vivo in the spinal cord, the brain, or the plasma of EAE mice receiving the NAAA inhibitor AM11095. Conversely, administration of the FAAH inhibitor PF-3845 and the dual NAAA-FAAH inhibitor AM11078 leads to an increase in AEA, PEA, OEA, and SEA levels in vivo. An influence of the time of sacrifice can be fairly excluded here, as we administered chronically the NAAA inhibitor to the mice and sacrificed the mice 1 h after the last administration, a timing already used in the literature with a NAAA inhibitor [25]. Besides, the NAAA inhibitor AM11095 is reported to be brain permeable and, when using this inhibitor, Sagheddu and colleagues observed, in naïve mice, increased PEA and OEA levels in specific regions of the brain 2 h post administration [27]. Indeed, the authors found a slight increase for OEA and PEA in the hippocampus and for OEA only in the cortex while these NAEs remained unchanged in the midbrain and striatum [27]. This may suggest that NAAA inhibition leads to region-specific alterations in NAE levels.

It should be noted that, contrary to FAAH inhibition, NAAA inhibition is generally associated with a relatively modest increase in NAE levels (e.g., [25, 27, 29]). Moreover, another group reported decreased NAAA activity but no changes in NAE levels upon administration of a NAAA inhibitor [53]. This could suggest the presence of a compensatory mechanism able to hydrolyze NAEs upon NAAA inhibition or the fact that the enzyme regulates a smaller but biologically relevant pool of NAEs. Therefore, besides

CNS region-specific variations of NAE levels, we can also hypothesize that NAAA inhibition increases NAEs in specific cells and/or in specific subcellular regions. Indeed, a specific increase in NAE levels in immune cells could reduce their activation. Moreover, NAAA inhibition could lead only to a slight increase in NAEs but in specific subcellular regions close to targets allowing for rapid physiological responses. A last point to mention related to NAAA inhibition is that we cannot rule out that, besides acting on NAEs, NAAA could hydrolyze yet-to-be identified substrates that could be relevant to the EAE disease.

In our hands, inhibiting both NAAA and FAAH in the context of EAE had no added value on the beneficial effects of NAAA inhibition alone. This is supported by the effects we observed using AM11078 (a dual NAAA-FAAH inhibitor) as well as a co-administration of the NAAA and FAAH inhibitors. An explanation might be the involvement of different NAEs. Indeed, depending on substrate preference, NAAA and FAAH inhibition could lead to increased levels of different NAE species in vivo. These lipids are mostly studied for their pro-homeostatic and anti-inflammatory properties. They can bind different receptors, including PPARα or CB_2 known to have beneficial effects in inflammatory processes [37, 54]. However, AEA or OEA can activate TRPV1 that can have deleterious effects in some settings [55]. For instance, a study comparing wild type and TRPV1-deficient mice in the EAE model supports deleterious effects of TRPV1 [56]. The authors also reported a risk association between a single nucleotide polymorphism in TRPV1 gene and primary progressive MS [56]. Nevertheless, the implication of TRPV1 activation in MS remains unclear. Indeed another study found an association between a mutation in the gene encoding for TRPV1, known to result in increased protein expression and function, and lower cerebrospinal fluid levels of TNF-α in MS patients [57]. They also reported that, in vitro, TRPV1 activation reduced cytokine production in microglial cells [57]. Another important aspect is the subcellular localization of the two enzymes. Indeed, NAAA is a lysosomal enzyme while FAAH is an endoplasmic reticulum-localized enzyme [20]. Therefore, depending on the subcellular localization of the increase in NAE levels, these bioactive lipids could initiate different signaling pathways (e.g., AEA could activate TRPV1 at the membrane level or PPARγ in the nucleus hence generating a different response).

Another point that could explain the lack of effects observed when using the FAAH inhibitor could be that FAAH hydrolyzes other substrates that would exert deleterious effects in EAE settings and therefore mitigate the beneficial effect of NAEs. To address this question, we thought to assess the properties of other known substrates of FAAH, namely *N*-acyltaurines and *N*-acylglycines in vitro [47–49, 51]. Indeed, *N*-acyltaurines and *N*-acyglycines were shown to be metabolized by FAAH into fatty acids and taurine or glycine. Although these lipids are poorly studied and their implication in inflammation remains unknown, some *N*-acyltaurine species were reported to bind and mediate their effects through TRPV1 and TRPV4 [51], both receptors being associated with inflammatory processes. As mentioned, TRPV1 has controversial effects in MS [56, 57]. TRPV4 was described to induce neuronal injury and enhance the inflammatory response in a murine model of epilepsy through the activation of microglial cells and astrocytes [58]. Moreover, in a model of cuprizone induced demyelination, blocking the TRPV4 receptor alleviated demyelination and glial activation [59]. In vitro, apoptosis of oligodendrocytes induced by LPS-activated microglia was also alleviated using a TRPV4-antagonist [59]. However in our study, we found only modest pro-inflammatory effects for *N*-acyltaurines in the primary co-culture of astrocytes and microglia.

One less-studied alternative to consider is the decrease of potentially anti-inflammatory FAAH products (e.g., taurine) when inhibiting this enzyme. Indeed, when working with FAAH inhibition, the focus is on increasing the levels of its substrates. However, FAAH inhibition would lead to decreased levels of the hydrolysis products, i.e., not only fatty acids but also ethanolamine for NAEs or taurine for *N*-acyltaurines. Indeed, taurine was demonstrated to be beneficial in inflammatory and neurological disorders (e.g., Alzheimer's disease; traumatic brain injury) [60] and was shown in vitro to enhance the process of drug-induced oligodendrocyte precursor cell differentiation and maturation [61]. Whether this could possibly also explain the differential effects observed between FAAH and NAAA inhibition remains to be explored.

Finally, the administration of AM11078 (the dual NAAA-FAAH inhibitor) showed less beneficial effects than the co-administration of the NAAA inhibitor (AM11095) and the FAAH inhibitor (PF-3845). As both AM11078 and AM11095 have similar in vivo potency in inhibiting NAAA, one explanation for the differences in effect could be different pharmacokinetic profiles. While our data in the EAE model do not support the interest of a dual inhibition, it remains to be seen whether this strategy could be of interest in other inflammatory diseases were increasing NAE levels is of interest (e.g., colitis, arthritis).

In conclusion, while our data support the beneficial effects of NAAA inhibition in this model of MS, potentially through modulation of resident immune cell activation, further studies will be needed to fully understand the differences we observed when inhibiting FAAH and NAAA or FAAH alone.

Supplementary Information The online version contains supplementary material available at https://doi.org/10.1007/s13311-021-01074-x.

Acknowledgements The MASSMET platform (UCLouvain, Belgium) is acknowledged for the access to the LC-MS. PB is a research fellow of the "Fonds pour la Recherche dans l'Industrie et l'Agriculture" (FRIA, Belgium). OGL and MA are postdoctoral fellows from the "Fonds de la Recherche Scientifique" (FRS-FNRS), Belgium.

Required Author Forms Disclosure forms provided by the authors are available with the online version of this article.

Funding The F.R.S.-FNRS, Belgium, and the Fondation Charcot, Belgium, provided grants to GGM for this research.

References

1. Dendrou CA, Fugger L, Friese MA. Immunopathology of multiple sclerosis. Nat Rev Immunol. 2015;15(9):545-58.
2. Li C, Wu X, Liu S, Shen D, Zhu J, Liu K. Role of Resolvins in the Inflammatory Resolution of Neurological Diseases. Front Pharmacol. 2020;11:612.
3. Ernest James Phillips T, Maguire E. Phosphoinositides: Roles in the Development of Microglial-Mediated Neuroinflammation and Neurodegeneration. Front Cell Neurosci. 2021;15:652593.
4. Alhouayek M, Ameraoui H, Muccioli GG. Bioactive lipids in inflammatory bowel diseases - From pathophysiological alterations to therapeutic opportunities. Biochim Biophys Acta Mol Cell Biol Lipids. 2021;1866(2):158854.
5. Tao X, Lee MS, Donnelly CR, Ji RR. Neuromodulation, Specialized Proresolving Mediators, and Resolution of Pain. Neurotherapeutics. 2020;17(3):886-99.
6. Portavella M, Rodriguez-Espinosa N, Galeano P, Blanco E, Romero JI, Holubiec MI, et al. Oleoylethanolamide and Palmitoylethanolamide Protect Cultured Cortical Neurons Against Hypoxia. Cannabis Cannabinoid Res. 2018;3(1):171-8.
7. Scuderi C, Stecca C, Valenza M, Ratano P, Bronzuoli MR, Bartoli S, et al. Palmitoylethanolamide controls reactive gliosis and exerts neuroprotective functions in a rat model of Alzheimer's disease. Cell Death Dis. 2014;5:e1419.
8. Schurman LD, Lichtman AH. Endocannabinoids: A Promising Impact for Traumatic Brain Injury. Front Pharmacol. 2017;8:69.
9. Petrosino S, Di Marzo V. The pharmacology of palmitoylethanolamide and first data on the therapeutic efficacy of some of its new formulations. Br J Pharmacol. 2017;174(11):1349-65.
10. Hernangomez M, Mestre L, Correa FG, Loria F, Mecha M, Inigo PM, et al. CD200-CD200R1 interaction contributes to neuroprotective effects of anandamide on experimentally induced inflammation. Glia. 2012;60(9):1437-50.
11. Gonzalez-Aparicio R, Blanco E, Serrano A, Pavon FJ, Parsons LH, Maldonado R, et al. The systemic administration of oleoylethanolamide exerts neuroprotection of the nigrostriatal system in experimental Parkinsonism. Int J Neuropsychopharmacol. 2014;17(3):455-68.
12. Beggiato S, Tomasini MC, Ferraro L. Palmitoylethanolamide (PEA) as a Potential Therapeutic Agent in Alzheimer's Disease. Front Pharmacol. 2019;10:821.
13. Siracusa R, Paterniti I, Impellizzeri D, Cordaro M, Crupi R, Navarra M, et al. The Association of Palmitoylethanolamide with Luteolin Decreases Neuroinflammation and Stimulates Autophagy in Parkinson's Disease Model. CNS Neurol Disord Drug Targets. 2015;14(10):1350-65.
14. Esposito E, Impellizzeri D, Mazzon E, Paterniti I, Cuzzocrea S. Neuroprotective activities of palmitoylethanolamide in an animal model of Parkinson's disease. PLoS One. 2012;7(8):e41880.
15. Rahimi A, Faizi M, Talebi F, Noorbakhsh F, Kahrizi F, Naderi N. Interaction between the protective effects of cannabidiol and palmitoylethanolamide in experimental model of multiple sclerosis in C57BL/6 mice. Neuroscience. 2015;290:279-87.
16. Loria F, Petrosino S, Mestre L, Spagnolo A, Correa F, Hernangomez M, et al. Study of the regulation of the endocannabinoid system in a virus model of multiple sclerosis reveals a therapeutic effect of palmitoylethanolamide. Eur J Neurosci. 2008;28(4):633-41.
17. Orefice NS, Alhouayek M, Carotenuto A, Montella S, Barbato F, Comelli A, et al. Oral Palmitoylethanolamide Treatment Is Associated with Reduced Cutaneous Adverse Effects of Interferon-beta1a and Circulating Proinflammatory Cytokines in Relapsing-Remitting Multiple Sclerosis. Neurotherapeutics. 2016;13(2):428-38.
18. Ueda N, Tsuboi K, Uyama T. Metabolism of endocannabinoids and related N-acylethanolamines: canonical and alternative pathways. FEBS J. 2013;280(9):1874-94.
19. Muccioli GG. Endocannabinoid biosynthesis and inactivation, from simple to complex. Drug Discov Today. 2010;15(11-12):474-83.
20. Bottemanne P, Muccioli GG, Alhouayek M. N-acylethanolamine hydrolyzing acid amidase inhibition: tools and potential therapeutic opportunities. Drug Discov Today. 2018;23(8):1520-9.
21. Piomelli D, Scalvini L, Fotio Y, Lodola A, Spadoni G, Tarzia G, et al. N-Acylethanolamine Acid Amidase (NAAA): Structure, Function, and Inhibition. J Med Chem. 2020.
22. Webb M, Luo L, Ma JY, Tham CS. Genetic deletion of Fatty Acid Amide Hydrolase results in improved long-term outcome in chronic autoimmune encephalitis. Neurosci Lett. 2008;439(1):106-10.
23. Rossi S, Furlan R, De Chiara V, Muzio L, Musella A, Motta C, et al. Cannabinoid CB1 receptors regulate neuronal TNF-alpha effects in experimental autoimmune encephalomyelitis. Brain Behav Immun. 2011;25(6):1242-8.
24. Pryce G, Cabranes A, Fernandez-Ruiz J, Bisogno T, Di Marzo V, Long JZ, et al. Control of experimental spasticity by targeting the degradation of endocannabinoids using selective fatty acid amide hydrolase inhibitors. Mult Scler. 2013;19(14):1896-904.
25. Migliore M, Pontis S, Fuentes de Arriba AL, Realini N, Torrente E, Armirotti A, et al. Second-Generation Non-Covalent NAAA Inhibitors are Protective in a Model of Multiple Sclerosis. Angew Chem Int Ed Engl. 2016;55(37):11193–7.
26. Malamas MS, Farah SI, Lamani M, Pelekoudas DN, Perry NT, Rajarshi G, et al. Design and synthesis of cyanamides as potent and selective N-acylethanolamine acid amidase inhibitors. Bioorg Med Chem. 2020;28(1):115195.
27. Sagheddu C, Scherma M, Congiu M, Fadda P, Carta G, Banni S, et al. Inhibition of N-acylethanolamine acid amidase reduces nicotine-induced dopamine activation and reward. Neuropharmacology. 2019;144:327-36.
28. Orefice NS, Guillemot-Legris O, Capasso R, Bottemanne P, Hantraye P, Caraglia M, et al. miRNA profile is altered in a modified EAE mouse model of multiple sclerosis featuring cortical lesions. Elife. 2020;9.
29. Alhouayek M, Bottemanne P, Subramanian KV, Lambert DM, Makriyannis A, Cani PD, et al. N-Acylethanolamine-hydrolyzing acid amidase inhibition increases colon N-palmitoylethanolamine levels and counteracts murine colitis. FASEB J. 2015;29(2):650-61.
30. Guillemot-Legris O, Masquelier J, Everard A, Cani PD, Alhouayek M, Muccioli GG. High-fat diet feeding differentially affects the development of inflammation in the central nervous system. J Neuroinflammation. 2016;13(1):206.
31. Mutemberezi V, Buisseret B, Masquelier J, Guillemot-Legris O, Alhouayek M, Muccioli GG. Oxysterol levels and metabolism in the course of neuroinflammation: insights from in vitro and in vivo models. J Neuroinflammation. 2018;15(1):74.
32. Alhouayek M, Bottemanne P, Makriyannis A, Muccioli GG. N-acylethanolamine-hydrolyzing acid amidase and fatty acid amide hydrolase inhibition differentially affect N-acylethanolamine

levels and macrophage activation. Biochim Biophys Acta Mol Cell Biol Lipids. 2017;1862(5):474-84.
33. De Berdt P, Bottemanne P, Bianco J, Alhouayek M, Diogenes A, Lloyd A, et al. Stem cells from human apical papilla decrease neuroinflammation and stimulate oligodendrocyte progenitor differentiation via activin-A secretion. Cell Mol Life Sci. 2018;75(15):2843-56.
34. Mutemberezi V, Masquelier J, Guillemot-Legris O, Muccioli GG. Development and validation of an HPLC-MS method for the simultaneous quantification of key oxysterols, endocannabinoids, and ceramides: variations in metabolic syndrome. Anal Bioanal Chem. 2016;408(3):733-45.
35. Contarini G, Giusti P, Skaper SD. Active Induction of Experimental Autoimmune Encephalomyelitis in C57BL/6 Mice. Methods Mol Biol. 2018;1727:353-60.
36. Aharoni R, Globerman R, Eilam R, Brenner O, Arnon R. Titration of myelin oligodendrocyte glycoprotein (MOG) - Induced experimental autoimmune encephalomyelitis (EAE) model. J Neurosci Methods. 2021;351:108999.
37. Cristino L, Bisogno T, Di Marzo V. Cannabinoids and the expanded endocannabinoid system in neurological disorders. Nat Rev Neurol. 2020;16(1):9-29.
38. Di Marzo V. New approaches and challenges to targeting the endocannabinoid system. Nat Rev Drug Discov. 2018;17(9):623-39.
39. Ahn K, Johnson DS, Mileni M, Beidler D, Long JZ, McKinney MK, et al. Discovery and characterization of a highly selective FAAH inhibitor that reduces inflammatory pain. Chem Biol. 2009;16(4):411-20.
40. Lassmann H. Pathology of inflammatory diseases of the nervous system: Human disease versus animal models. Glia. 2020;68(4):830-44.
41. Frezel N, Sohet F, Daneman R, Basbaum AI, Braz JM. Peripheral and central neuronal ATF3 precedes CD4+ T-cell infiltration in EAE. Exp Neurol. 2016;283(Pt A):224-34.
42. Gobel K, Ruck T, Meuth SG. Cytokine signaling in multiple sclerosis: Lost in translation. Mult Scler. 2018;24(4):432-9.
43. Zilkha-Falb R, Rachutin-Zalogin T, Cleaver L, Gurevich M, Achiron A. RAM-589.555 favors neuroprotective and anti-inflammatory profile of CNS-resident glial cells in acute relapse EAE affected mice. J Neuroinflammation. 2020;17(1):313.
44. Griffin P, Dimitry JM, Sheehan PW, Lananna BV, Guo C, Robinette ML, et al. Circadian clock protein Rev-erbalpha regulates neuroinflammation. Proc Natl Acad Sci U S A. 2019;116(11):5102-7.
45. Tintore M, Vidal-Jordana A, Sastre-Garriga J. Treatment of multiple sclerosis - success from bench to bedside. Nat Rev Neurol. 2019;15(1):53-8.
46. Fletcher JM, Lalor SJ, Sweeney CM, Tubridy N, Mills KH. T cells in multiple sclerosis and experimental autoimmune encephalomyelitis. Clin Exp Immunol. 2010;162(1):1-11.
47. Long JZ, LaCava M, Jin X, Cravatt BF. An anatomical and temporal portrait of physiological substrates for fatty acid amide hydrolase. J Lipid Res. 2011;52(2):337-44.
48. Bradshaw HB, Rimmerman N, Hu SS, Benton VM, Stuart JM, Masuda K, et al. The endocannabinoid anandamide is a precursor for the signaling lipid N-arachidonoyl glycine by two distinct pathways. BMC Biochem. 2009;10:14.
49. Leishman E, Cornett B, Spork K, Straiker A, Mackie K, Bradshaw HB. Broad impact of deleting endogenous cannabinoid hydrolyzing enzymes and the CB1 cannabinoid receptor on the endogenous cannabinoid-related lipidome in eight regions of the mouse brain. Pharmacol Res. 2016;110:159-72.
50. Sasso O, Pontis S, Armirotti A, Cardinali G, Kovacs D, Migliore M, et al. Endogenous N-acyl taurines regulate skin wound healing. Proc Natl Acad Sci U S A. 2016;113(30):E4397-406.
51. Saghatelian A, McKinney MK, Bandell M, Patapoutian A, Cravatt BF. A FAAH-regulated class of N-acyl taurines that activates TRP ion channels. Biochemistry. 2006;45(30):9007-15.
52. Correa F, Hernangomez-Herrero M, Mestre L, Loria F, Docagne F, Guaza C. The endocannabinoid anandamide downregulates IL-23 and IL-12 subunits in a viral model of multiple sclerosis: evidence for a cross-talk between IL-12p70/IL-23 axis and IL-10 in microglial cells. Brain Behav Immun. 2011;25(4):736-49.
53. Li Y, Zhou P, Chen H, Chen Q, Kuang X, Lu C, et al. Inflammation-restricted anti-inflammatory activities of a N-acylethanolamine acid amidase (NAAA) inhibitor F215. Pharmacol Res. 2018;132:7-14.
54. Tsuboi K, Uyama T, Okamoto Y, Ueda N. Endocannabinoids and related N-acylethanolamines: biological activities and metabolism. Inflamm Regen. 2018;38:28.
55. Kong WL, Peng YY, Peng BW. Modulation of neuroinflammation: Role and therapeutic potential of TRPV1 in the neuro-immune axis. Brain Behav Immun. 2017;64:354-66.
56. Paltser G, Liu XJ, Yantha J, Winer S, Tsui H, Wu P, et al. TRPV1 gates tissue access and sustains pathogenicity in autoimmune encephalitis. Mol Med. 2013;19:149-59.
57. Stampanoni BM, Gentile A, Iezzi E, Zagaglia S, Musella A, Simonelli I, et al. Transient Receptor Potential Vanilloid 1 Modulates Central Inflammation in Multiple Sclerosis. Front Neurol. 2019;10:30.
58. Wang Z, Zhou L, An D, Xu W, Wu C, Sha S, et al. TRPV4-induced inflammatory response is involved in neuronal death in pilocarpine model of temporal lobe epilepsy in mice. Cell Death Dis. 2019;10(6):386.
59. Liu M, Liu X, Wang L, Wang Y, Dong F, Wu J, et al. TRPV4 Inhibition Improved Myelination and Reduced Glia Reactivity and Inflammation in a Cuprizone-Induced Mouse Model of Demyelination. Front Cell Neurosci. 2018;12:392.
60. Jakaria M, Azam S, Haque ME, Jo SH, Uddin MS, Kim IS, et al. Taurine and its analogs in neurological disorders: Focus on therapeutic potential and molecular mechanisms. Redox Biol. 2019;24:101223.
61. Beyer BA, Fang M, Sadrian B, Montenegro-Burke JR, Plaisted WC, Kok BPC, et al. Metabolomics-based discovery of a metabolite that enhances oligodendrocyte maturation. Nat Chem Biol. 2018;14(1):22-8.

Publisher's Note Springer Nature remains neutral with regard to jurisdictional claims in published maps and institutional affiliations.